# Quantitative Stress First-Pass Perfusion Cardiac MRI: State of the Art

*Roberta Catania, MD • Sandra Quinn, MBBCh, PhD • Amir A. Rahsepar, MD • Tugce Agirlar Trabzonlu, MD • Jay B. Bisen, BS*
*Kelvin Chow, PhD • Daniel C. Lee, MD • Ryan Avery, MD • Peter Kellman, PhD • Bradley D. Allen, MD, MS*

Author affiliations, funding, and conflicts of interest are listed at the end of this article.
See the invited commentary by Leung and Ng in this issue.

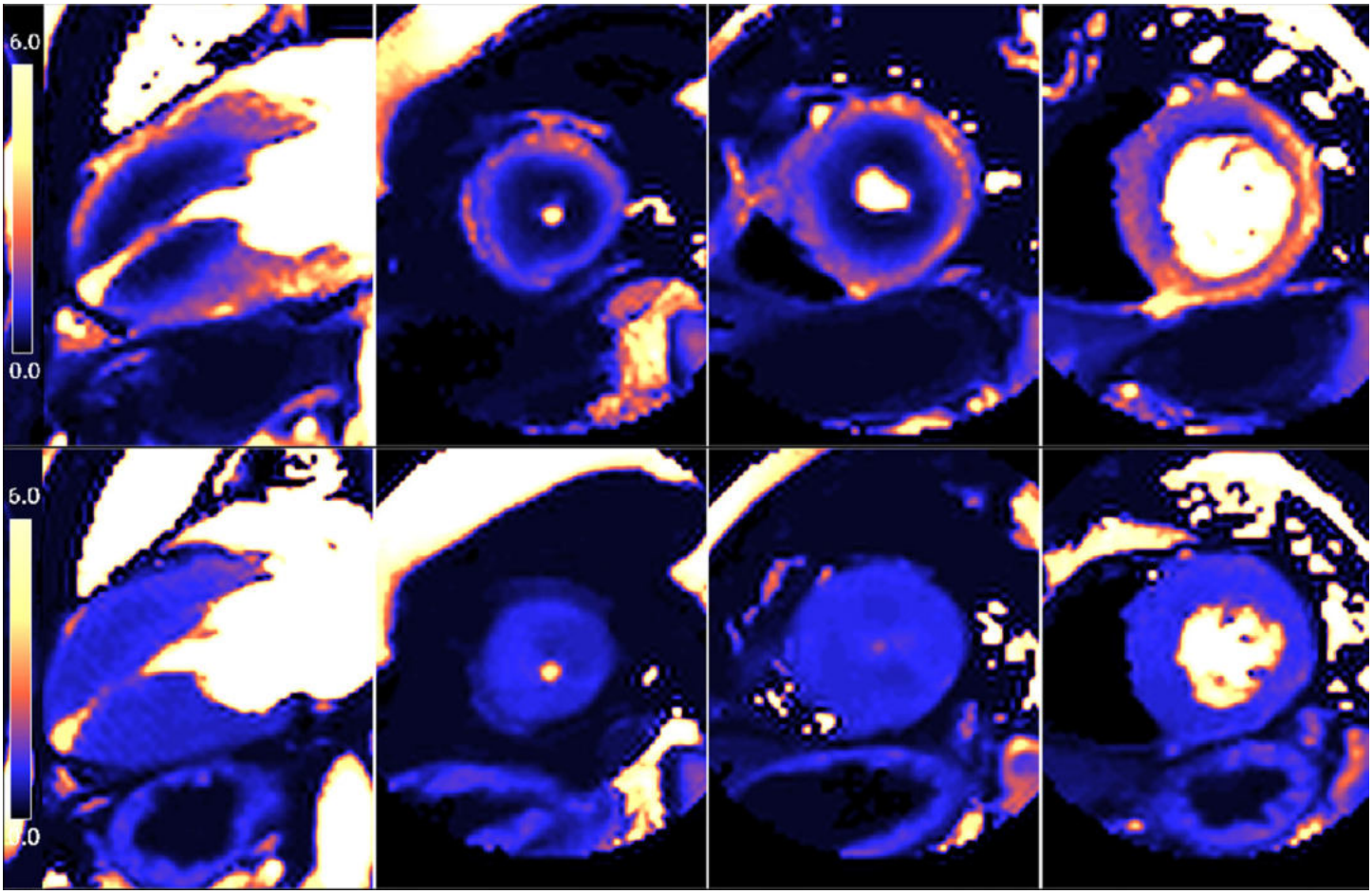


Quantitative stress perfusion (qPerf) cardiac magnetic resonance (CMR) imaging is a noninvasive approach used to quantify myocardial blood flow (MBF). Compared with visual analysis, qPerf CMR has superior diagnostic accuracy in the detection of myocardial ischemia and assessment of ischemic burden. In the evaluation of epicardial coronary artery disease (CAD), qPerf CMR improves the distinction of single-vessel from multivessel disease, yielding a more accurate estimate of the ischemic burden, and in turn improving patient management. In patients with chest pain without epicardial CAD, the findings of lower stress MBF and myocardial perfusion reserve (MPR) allow the diagnosis of microvascular dysfunction (MVD). Given its accuracy, MBF quantification with stress CMR has been introduced into the most recent recommendations for diagnosis in patients who have ischemia with nonobstructive CAD. Recent studies have shown a greater decrease in stress MBF and MPR in patients with three-vessel CAD compared with those in patients with MVD, demonstrating an important role that quantitative stress CMR can play in differentiating these etiologies in patients with stable angina. In cases of hypertrophic cardiomyopathy and cardiac amyloidosis, qPerf CMR aids in early diagnosis of ischemia and in risk assessment. Ischemia also results from alterations in hemodynamics that may occur with valve disease such as aortic stenosis or in cases of heart failure. qPerf CMR has emerged as a useful noninvasive tool for detection of cardiac allograft vasculopathy in patients who have undergone heart transplant. The authors review the basic principles and current primary clinical applications of qPerf CMR.



RG

CARDIAC IMAGING

Invited Commentary Supplemental Material TestYour Knowledge CME

**RadioGraphics 2025; 45(3):e240115**
**https://doi.org/10.1148/rg.240115**

**Content Codes:** CA, MR

**Abbreviations:** AIF = arterial input function, AUC = area under receiver operating characteristic curve, CAD = coronary artery disease, CAV = cardiac allograft vasculopathy, CMR = cardiac magnetic resonance, GBCA = gadolinium-based contrast agent, HCM = hypertrophic cardiomyopathy, ICA = invasive coronary angiography, LGE = late gadolinium enhancement, MBF = myocardial blood flow, MPR = myocardial perfusion reserve, MVD = microvascular dysfunction, qPerf = quantitative stress perfusion, SBP = systolic blood pressure, SSO = splenic switch-off

## TEACHING POINTS

- In studies on quantitative CMR with invasive coronary angiography (ICA) as the reference standard, average normal rest MBF values of between 0.8 and 1.3 mL/min/g, average normal stress MBF values of between 2.3 and 3.7 mL/min/g, and average normal MPR values of between 2.6 and 4.1 have been reported.
- The most important added value of qPerf imaging is based on its greater capability in distinguishing single-vessel from multivessel disease.
- While stress MBF of 2.25 mL/g/min or greater can be used to differentiate normal from abnormal (either obstructive CAD or MVD) blood flow with high accuracy (AUC, 0.96), stress MBF of 1.82 mL/g/min or lower can be used to differentiate obstructive three-vessel CAD from MVD (AUC, 0.99).
- Perfusion defects have been reported in both the hypertrophied myocardium and normal myocardium, and qPerf CMR may be an early assessment tool in HCM gene mutation carriers.
- qPerf CMR can help to assess for inadequate vasodilator response with decreased stress MBF and MPR. These findings can also mimic myocardial perfusion defects. However, in the setting of inadequate response, stress MBF will be nearly identical to rest MBF, with the MPR close to 1.0.

## Introduction

Stress perfusion cardiac magnetic resonance (CMR) imaging is an established noninvasive examination for the diagnosis of obstructive coronary artery disease (CAD) (1). Among noninvasive imaging modalities, PET and stress perfusion CMR have the highest combination of sensitivity and specificity to detect anatomically and functionally significant CAD (2). Furthermore, stress perfusion CMR provides prognostic information and can serve as a gatekeeper for cardiac catheterization in patients suspected of having CAD (3). In addition, perfusion imaging can be incorporated into other CMR techniques for comprehensive assessment of cardiac structure, function, viability, tissue characterization, and blood flow velocities in a single examination (2).

Beyond the visual assessment of perfusion defects, techniques have been developed to provide fully quantitative evaluation of myocardial blood flow (MBF, in mL/min/g) using stress perfusion CMR and have been shown to improve diagnostic accuracy of stress perfusion CMR. Quantification of MBF with use of CMR is particularly well suited for the evaluation of microvascular dysfunction (MVD), and as a result, it is now included in the recommendations for diagnostic testing in patients suspected of having ischemia with nonobstructive CAD (4).

In this article, the authors review the state of the art in fully quantitative stress perfusion (qPerf) CMR, including the basic principles and main clinical applications of this examination. This review is focused on true quantitative techniques (as opposed to semiquantitative methods), with attention to the most studied diseases, including epicardial CAD, ischemia with nonobstructive CAD, MVD in nonobstructive cardiomyopathy with a focus on hypertrophic cardiomyopathy (HCM) and amyloidosis, and cardiac allograft vasculopathy (CAV) after heart transplant. The authors also discuss situations that may lead to the misinterpretation of qPerf CMR findings and provide recommendations for troubleshooting.

## Myocardial Blood Flow

MBF is a critical aspect of cardiac function, and understanding the basic physiology of MBF is fundamental to the adequate interpretation of normal and pathologic findings of qPerf CMR. This interpretation process involves the coordinated response of epicardial coronary arteries, prearterioles, and arterioles to numerous stimuli, including neural, hormonal, and local metabolic factors; tissue compressive forces; and coronary perfusion pressures. This process results in the regulation of coronary vascular resistance and ultimately creates a continuous supply of oxygen and nutrients to meet the high and varying metabolic demands of the myocardium (5).

MBF is primarily determined by the epicardial coronary arteries, which serve as the primary capacitance conduits of oxygenated blood to the myocardium and further branch into prearterioles (most responsive to pressure changes) and arterioles (responsive to the metabolic regulation) and ultimately into capillaries, forming an extensive microvascular network throughout the myocardium (Fig 1) (6,7).

At rest, MBF remains constant over a wide range of perfusion pressures due to coronary vascular resistance autoregulation by the arterial microvasculature (7,8). Since at rest up to 80% of coronary blood oxygen is already extracted, when the metabolic demand increases (eg, during exercise), the myocardium relies on nearly immediate increases in MBF to meet the increased oxygen demand (7). Vasodilation occurs mostly at the level of the arterioles in response to this demand. As a result, under stress conditions, the MBF can increase up to four- to fivefold to respond to the increased oxygen demand (Fig 2A). The increased coronary flow achievable from basal perfusion to maximal vasodilatation corresponds to the myocardial perfusion reserve (MPR), which is calculated as the MBF at stress divided by the MBF at rest.

In epicardial CAD, autoregulation of microvascular tone maintains adequate resting myocardial perfusion pressure despite obstructive stenosis, but at the expense of the vasodilator reserve. Maximal MBF augmentation will be diminished and MBF will be insufficient to meet demand, resulting in myocardial ischemia (Fig 2B). With MVD, there is loss of microvasculature dilation capability due to multiple different causes (eg, hypertension, diabetes), resulting in impaired stress MBF and MPR (Fig 2C), even in the absence of significant epicardial CAD (Table 1) (7–9). The endocardium experiences greater perfusion limitations than the epicardium due to the longer intramural path that arteries must

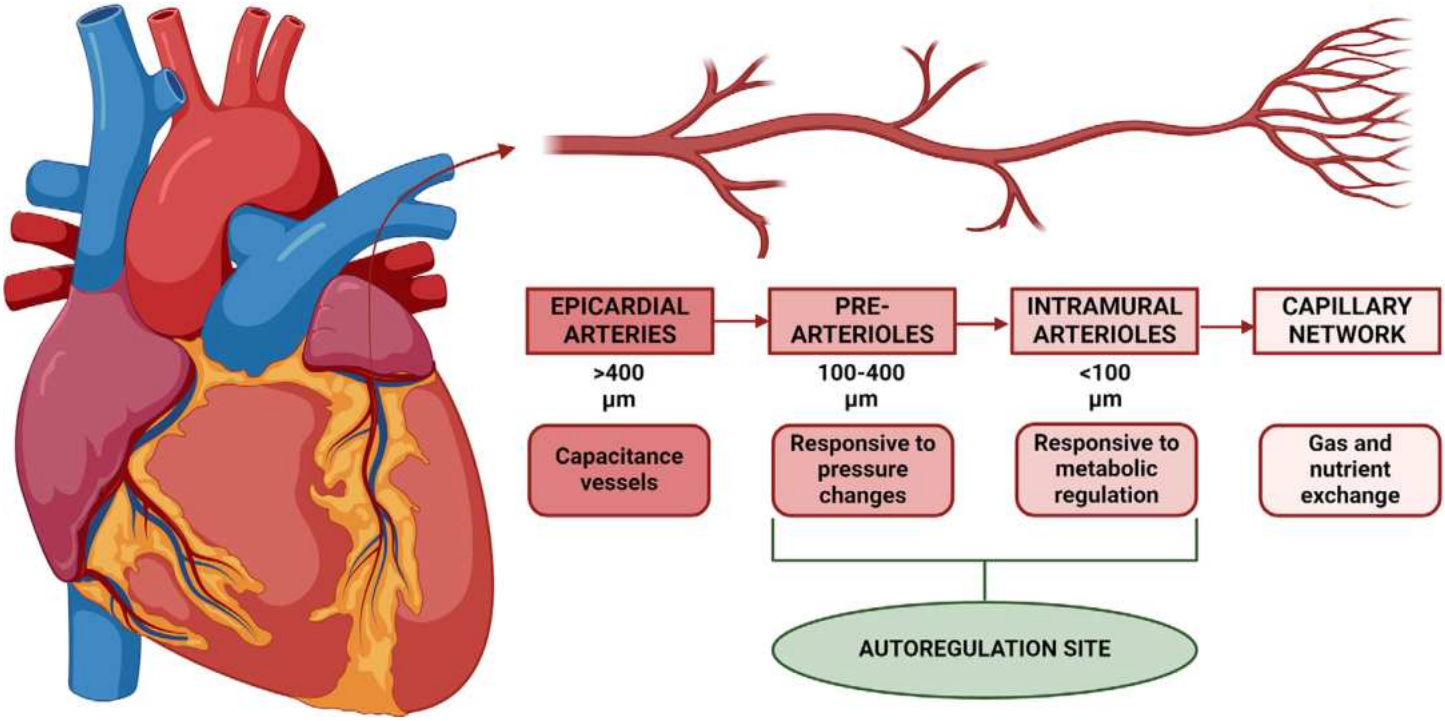


**Figure 1.** Drawing illustrates the coronary circulation. Epicardial arteries serve as conduit arteries. Prearterioles can regulate their diameter in response to pressure changes (myogenic response). Intramural arterioles are sensitive to metabolic changes (7).

traverse, delayed early diastolic microcirculatory perfusion, and higher compressive forces from intraventricular diastolic pressure. Under normal conditions, these effects are offset by an autoregulatory decrease in subendocardial microvascular resistance. Vasodilator reserve is consequently reduced, and susceptibility to ischemia is increased in the endocardium relative to the epicardium. During vasodilator stress, increasing degrees of coronary artery stenosis will increase the transmural perfusion gradient, resulting in subendocardial hypoperfusion (7,8).

### Stress Agents

Stress agents (vasodilator or inotropic) administered during stress perfusion CMR induce pharmacologic stress and unmask the presence of myocardial ischemia. Although a detailed discussion of this phenomenon is beyond the scope of this article, the fundamentals of the most commonly used stress agents are briefly summarized in Table 2.

Adenosine, a vasodilator, mainly activates A1, A2b, and A3 receptors. This stress agent has a short half-life (~10 seconds), making it ideal for controlled stress induction (10). Caution is warranted, as the use of adenosine is contraindicated in cases of second- or third-degree atrioventricular block, systolic blood pressure (SBP) lower than 90 mm Hg, uncontrolled reactive airway disease, sinus bradycardia with a heart rate lower than 40 beats per minute, and hypersensitivity. Furthermore, the administration of adenosine and gadolinium-based contrast agent requires two intravenous access sites in contralateral arms.

Regadenoson is another vasodilator that is a specific A2a receptor agonist (11). The longer elimination phase for regadenoson, as compared with that for adenosine, is noteworthy. When rest images are acquired, the use of regadenoson requires an antagonist agent (aminophylline) to be administered immediately after the stress image acquisition by means of slow intravenous injection for 30–60 seconds at a dose of 50–250 mg. The advantage of using regadenoson is that it can be administered as a single bolus without two separate venous accesses being required. However, despite the use of an antagonist agent, the vasodilator effect can persist during rest acquisition, leading to an overestimation of resting MBF and an underestimation of the MPR (12).

Inotropic stress agents such as dobutamine stimulate β1 and β2 receptors, providing more physiologic stress. Dobutamine is preferred for stress echocardiography and is considered a second-line option for other myocardial perfusion imaging examinations (13). Contraindications to these stress agents include arrhythmias, history of recent myocardial infarction, left ventricular outflow tract obstruction, and aortic dissection.

## Stress CMR Protocol

A typical stress CMR protocol includes *(a)* stress perfusion, *(b)* rest perfusion, *(c)* late gadolinium enhancement (LGE), and *(d)* short-axis cine imaging. While the primary objective of stress CMR is ischemia evaluation, an important strength of this examination is the capability to yield additional quantitative and qualitative information that provides an important context in the diagnosis or risk stratification of patients. These applications may include left and right ventricle volumetric and functional assessments (including strain), myocardial tissue characterization with T1 and T2 mapping and LGE imaging, aorta or other vascular assessments, and quantitative evaluation of blood flow and velocities if necessary for assessment of valvular heart disease (14).

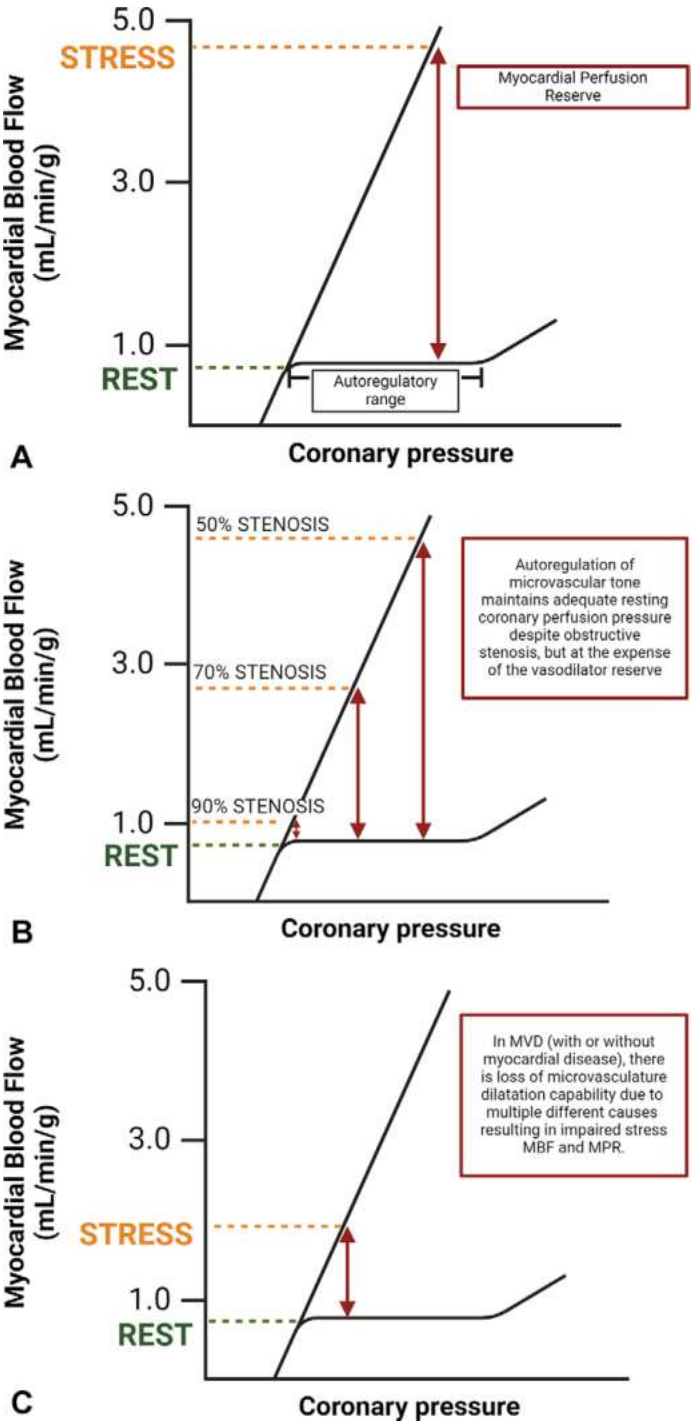


**Figure 2.** Physiology of MBF. **(A)** The normal myocardium already extracts 80% of oxygen at rest. Coronary autoregulation allows an up to four- to fivefold increase in MBF in response to increased oxygen demand. The increased coronary flow that is achievable during basal perfusion to maximal vasodilatation is the myocardial perfusion reserve (MPR [red arrows]). **(B)** In the presence of epicardial CAD, autoregulation maintains adequate resting myocardial perfusion at the expense of the MPR (red arrows), which then results in ischemia when the MBF is insufficient to meet demand. **(C)** With MVD, which can occur with or without myocardial disease (eg, HCM, amyloidosis), there is loss of microvascular dilation capability, resulting in impaired stress MBF and MPR, even in the absence of significant epicardial CAD (7). Red arrows indicate MPR, orange dashed lines indicate stress MBF, and green dashed lines indicate rest MBF.

**Table 1: Classification of Myocardial Vascular Dysfunction**

| |
|---|
| Epicardial coronary arteries |
| Atherosclerotic disease |
| Vasospastic disease |
| Coronary microcirculation |
| With myocardial disease |
| HCM |
| Dilated cardiomyopathy |
| Amyloidosis |
| Other disorders |
| Without myocardial disease |

Sources.—References 7 and 8.

The stress perfusion CMR protocol used at our institution is outlined in Figure 3 (15–19). Initially, localizer and full–field-of-view precontrast images of the chest are obtained. Long-axis balanced steady-state free-precession cine images in two-, three-, and four-chamber views, as well as T1 and T2 mapping, are obtained before contrast material is administered. Gadolinium-based contrast agents (GBCAs) are used for myocardial flow and fibrosis detection owing to their shortening of T1 relaxation time (20,21). Stress and rest perfusion images are each acquired with a contrast agent bolus; thus, the total contrast agent dose, which is calculated on the basis of the patient's weight, is divided in half at a dose of 0.05–0.1 mmol/kg for each phase. Alternatively, the total dosage can be divided into three parts, with an additional smaller dose administered after rest imaging to improve the LGE images.

When adenosine is used, it is generally recommended to perform stress imaging first and allow sufficient time (~8–10 minutes) before rest imaging to allow the effect of the stress agent and contrast material within the blood pool to subside. To optimize the acquisition time, we obtain our short-axis stack of balanced steady-state free-precession cine images between stress and rest perfusion image acquisitions. Stress imaging only (without rest imaging) can also be performed to enhance efficiency (22). The main disadvantage of using this approach in the setting of qPerf imaging is that the MPR cannot be quantified without rest MBF. In general, acquiring stress images before rest images is recommended to optimize workflow and allow ischemia evaluation in the rare circumstance that a patient cannot complete the remainder of the examination.

After the completion of rest imaging, it is important to allow ample time for the contrast agent to "wash in" to the myocardium for adequate LGE imaging. Ideally, there should be at least 10 minutes between the GBCA injection and LGE imaging. However, because of the divided GBCA dose between the stress and rest image acquisitions, phase-sensitive inversion-recovery (PSIR) LGE imaging can be performed 5–7 minutes after rest imaging (~15 minutes after stress imaging). During this 5–7-minute interval, additional postcontrast full–field-of-view imaging, phase contrast imaging, or angiography can be performed. Postcontrast T1 mapping can be performed after LGE imaging to allow extracellular volume quantification.

**Table 2: Most Common Stress Agents**

| Stress Agent | Mechanism of Action | Dose | Pros | Cons | Side Effects |
|---|---|---|---|---|---|
| Adenosine | Vasodilator<br>Activation of A1, A2a, A2b, and A3 receptors | 140 μg/kg/min for 2–4 min<br>Can be increased up to 210 μg/kg/min if there is no 10-bpm HR increase or >10-mm Hg SBP decrease | Short half-life (10 sec) | Caffeine intake within 12 h before the examination<br>2nd- or 3rd-degree AV block<br>SBP <90 mm Hg<br>Severe systemic arterial hypertension (>220/120 mm Hg)<br>Active airway disease<br>Hypersensitivity<br>Requires two intravenous accesses | Expected: flushing, chest pain, palpitations, breathlessness<br>More severe: heart blockage, transient hypotension, bronchospasm |
| Regadenoson | Vasodilator<br>A2a receptor agonist | Single 0.4-mg dose injection | Single intravenous access | Similar to adenosine<br>Longer elimination phase, which requires reversal (100 mg of aminophylline intravenously)<br>Action can persist after reversal | Expected: flushing, chest pain, palpitations, breathlessness<br>More severe: heart blockage, transient hypotension, bronchospasm |
| Dobutamine | Inotropic agent<br>Direct β1 and β2 receptor stimulation | 40 μg/kg/min | Greater physiologic stress | Uncontrolled AF, complex cardiac arrhythmias<br>Uncontrolled CHF<br>HOCM<br>Unstable angina<br>Severe aortic stenosis<br>Severe systemic arterial hypertension (>220/120 mm Hg)<br>β-blockers and nitrate intake within 12–24 h before the examination | Expected: chest pain, palpitations<br>More severe: myocardial infarction, VF, sVT |

Source.—Reference 14.
Note.—AF = atrial fibrillation, AV = atrioventricular, bpm = beats per minute, CHF = congestive heart failure, HOCM = hypertrophic obstructive cardiomyopathy, HR = heart rate, sVT = sustained ventricular tachycardia, VF = ventricular fibrillation.

## Stress Perfusion CMR Technique

Stress perfusion CMR involves the use of dynamic imaging to measure the kinetics of contrast agent uptake in the myocardium as a measure of MBF. Saturation-recovery techniques are commonly used to generate T1 contrast, with a gradient-echo or balanced steady-state free-precession readout (Table 3). ECG-gated and single-shot images with a typical temporal resolution of less than 100 msec are obtained and repeated at every heartbeat (14). Three short-axis imaging planes are common, but six short-axis or additional long-axis planes can be obtained by imaging each section at every other heartbeat. This alternating acquisition for additional planes reduces the temporal resolution of the myocardial signal that enables the advantage of greater spatial coverage, but it has been shown to be effective for quantitative perfusion mapping (23). The typical spatial resolution (2.5 $mm^2$) is in plane with an 8-mm section thickness, although higher acceleration rates or noncartesian readouts may improve the spatial resolution. Contrast agent injection rates can range from 3 to 7 mL/sec, with a 20–30-mL saline flush (14). While differences in T1 relaxivity of various GBCAs can impact image quality, no studies have evaluated the impact on MBF quantification.

Stress CMR is more commonly performed at 1.5 T, but data suggest that performing stress perfusion CMR at 3.0 T can improve image quality, decrease dark rim artifact, and result in high accuracy for qualitative and quantitative analyses (24–26). For qPerf analysis, an arterial input function (AIF) must be quantified at both stress and rest. The AIF is a dynamic measure of the left ventricle blood pool contrast signal intensity that is necessary for MBF quantification and can be used to estimate the absolute MBF with use of signal intensity and pharmacokinetic modeling. Due to nonlinear effects with large differences in contrast agent concentration in the blood pool and myocardium and T1 blunting of the contrast-enhanced blood pool, the AIF cannot be accurately quantified by using standard perfusion images. Instead, AIF quantification requires the use of a dedicated dual-sequence acquisition or dual-bolus approach. Both techniques are designed to reduce the left ventricle blood pool signal intensity and the associated saturation effects, providing more accurate AIF quantification. With the dual-sequence technique, low-spatial-resolution blood pool images are acquired with a shorter saturation-recovery time to minimize signal intensity saturation (27). These AIF images are acquired at every heartbeat and interleaved with high-resolution perfusion images during the same perfusion injection. The dual-sequence approach can be easily integrated into the clinical workflow.

The dual-bolus approach involves the use of a separate bolus injection of diluted (~1/10 concentration) GBCA to reduce the nonlinear saturation effects, enabling AIF quantification.

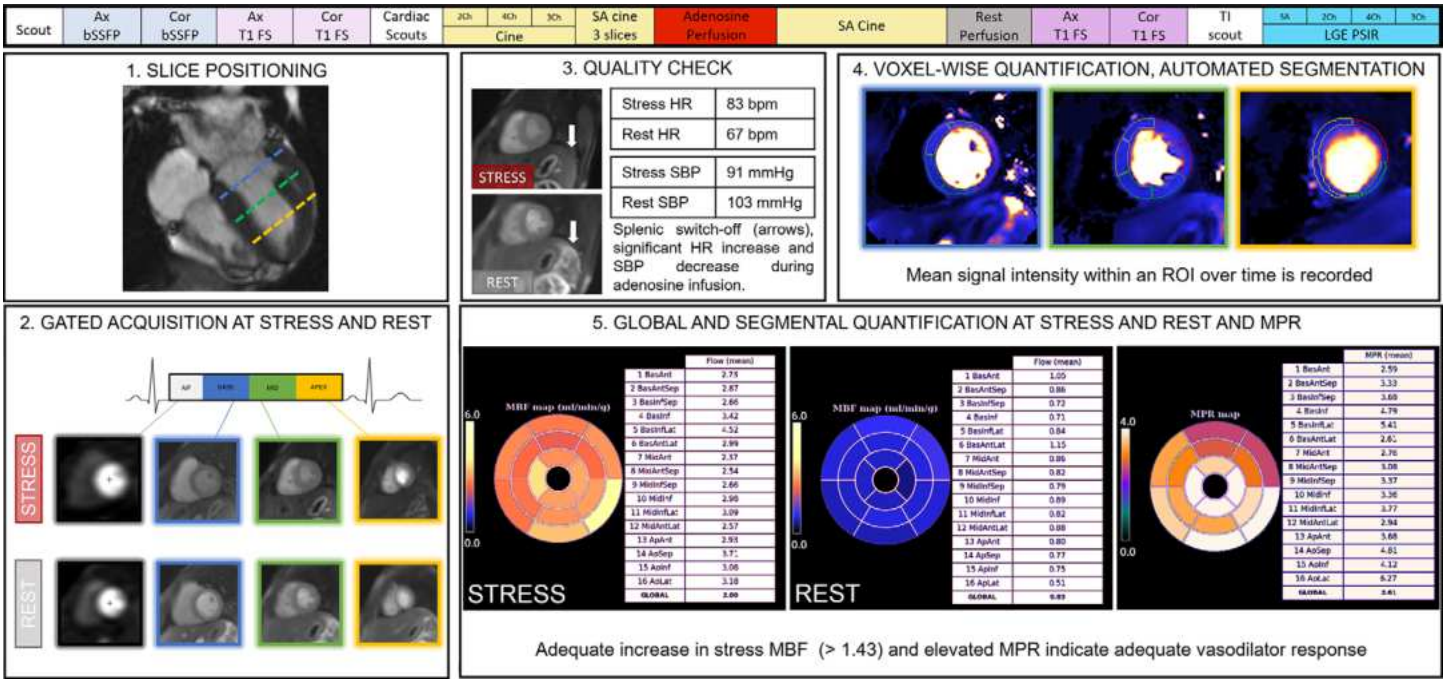


**Figure 3.** Stress adenosine perfusion protocol based on the protocol at the authors' institution. *1.* Slice positioning. Our standard practice is to use three slices, but six short-axis planes or long-axis planes can be imaged since they have been shown to increase diagnostic accuracy and reader confidence (15,16). *2.* Gated acquisition at stress and rest. Dual-bolus or dual-sequence techniques can be used to obtain arterial input function (AIF). *3.* Quality check. An adequate increase in stress MBF and an elevated MPR have had higher accuracy for detection of an adequate vasodilator response compared with heart rate *(HR)* and SBP changes and splenic switch-off (if adenosine is used) (17–19). *4.* Voxel-wise quantification and automated segmentation. *5.* Global and segmental MBF quantification at stress and rest and MPR. *Ax* = axial, *bSSFP* = balanced steady-state free precession, *Cor* = coronal, *FS* = fat saturated, *4ch* = four chambers, *PSIR* = phase-sensitive inversion recovery, *ROI* = region of interest, *SA* = short axis, *3ch* = three chambers, *TI* = inversion time, *2ch* = two chambers.

**Table 3: Pulse Sequence Parameters for 1.5-T Myocardial Perfusion CMR**

| Parameter | GRE (FLASH) | SSFP |
|---|---|---|
| TE (msec) | 1.00 | 1.04 |
| TR (msec) | 2.1 | 2.5 |
| Flip angle | 14° | 50° |
| Matrix | 192 × 111 | 192 × 111 |
| Imaging duration (msec) | 59 | 70 |
| Total duration per section (msec) | 143 | 142 |
| Three section + AIF (msec) | 497 (>120 bpm) | 495 (>120 bpm) |

Source.—Reference 22.
Note.—AIF = arterial input function, bpm = beats per minute, FLASH = fast low-angle shot, GRE = gradient echo, SSFP = steady-state free precession, TE = echo time, TR = repetition time.

A separate injection of full-concentration GBCA is then used for standard perfusion imaging (28).

Ideally, breath-hold sequences should be used to avoid motion artifacts. However, long breath holds can cause involuntary changes in heart rate and be difficult to achieve in patients who are experiencing pharmacologic stress. Thus, free-breathing acquisitions are preferred, with the application of motion-correction techniques that decrease motion artifacts for better quantification (28). Fully quantitative methods involve the use of a variety of models, all of which allow the conversion of dynamic MRI signal intensity changes over time into gadolinium-based contrast agent concentrations to provide stress and rest MBF measurements (in mL/min/g) (17,28,29). Fully automated postprocessing that yields stress and rest MBF measurements without additional time-consuming postprocessing is available (30,31).

Absolute MBF values may vary between CMR techniques (eg, dual-sequence vs dual-bolus). Differences in algorithm implementation may also result in differences between hardware and software vendors. These differences are not yet well characterized in the literature, although this is similarly true for non-CMR perfusion measurements. Comparisons of absolute values between studies performed with different acquisition or analysis approaches should be performed with caution, and clinical follow-up studies should be performed with the same techniques whenever possible.

Quantitative techniques performed with dual-bolus or dual-sequence techniques are discussed in the following sections, which serve as an insightful guide on how to interpret qPerf imaging findings in clinical practice.

## Perfusion CMR Interpretation

### Quality Check

Vasodilator response is typically assessed by observing an increase in heart rate and decrease in blood pressure during vasodilator agent infusion combined with the development

**Table 4: Qualitative Interpretation at Stress Perfusion CMR**

| Stress | Rest | LGE | Interpretation |
|---|---|---|---|
| – | – | – | Normal |
| + | – | – | Ischemia* |
| + | + | + | Infarct |
| + | + | – | Artifact* |

Note.—Stress, rest, and LGE CMR image interpretations are based on the presence (+) or absence (–) of perfusion defects. *An inducible perfusion defect first occurs when contrast material arrives in the left ventricle; then, it persists beyond peak myocardial enhancement and for several R-R intervals. The defect is more than two pixels wide (31).

of ischemic symptoms. Lack of this physiologic response during vasodilator infusion should raise suspicion for an inadequate response to pharmacologic vasodilator administration. Heart rate and blood pressure responses can vary according to patient sex and age (15), but an increase in heart rate of 10–15 beats per minute and a decrease in SBP greater than 10 mm Hg from the baseline should be observed (14). Due to denervation, patients who have undergone heart transplant will not have similar physiologic responses, so heart rate and blood pressure changes should not be used to assess vasodilator response in this group.

When adenosine is used, another useful tool for evaluating vasodilator response is the splenic switch-off (SSO). SSO manifests as nonenhancement of the spleen with GBCA infusion during adenosine administration (Fig 3, panel 3). The underlying mechanism of SSO is unclear, but it is presumably related to reduced splanchnic blood flow mediated by reactive sympathetic vasoconstriction after adenosine-induced hypotension (16). The absence of an SSO (ie, presence of splenic enhancement during stress), together with the absence of heart rate changes and SBP changes, may reflect a poor vasodilator response, which helps in identifying false-negative examination results at visual assessment or false-positive results at quantitative assessment. However, the sensitivity and specificity of SSO varies, and absence of SSO can sometimes occur in cases of adequate adenosine response (16). Moreover, SSO is used to assess the systemic response to adenosine rather than the direct effect to the heart. As discussed later (in the "Inadequate Vasodilator Response" section), MBF quantification itself can help in assessing appropriate vasodilator response and has been proven to be superior to blood pressure response, heart rate response, and SSO for evaluation of adequate stress response (32).

### Qualitative Interpretation

In our clinical practice, dynamic perfusion images are reviewed and analyzed together with LGE images (Table 4). The concomitant acquisition and interpretation of LGE images improve diagnostic accuracy for ischemia evaluation (33). A perfusion defect appears as a subendocardial or transmural area of hypoenhancement. A reversible defect is visible only at stress, with normal perfusion at rest and without associated delayed enhancement on LGE images. Perfusion defects occur early during myocardial contrast material arrival, persist beyond peak myocardial enhancement and for several R-R intervals, and are wider than two pixels (34). Also, it is good practice to scrutinize cine images for the presence of regional wall motion abnormalities that can help identify involved myocardial segments.

### Quantitative Interpretation

A normal vasodilator response results in an increased stress MBF. Based on studies using myocardial perfusion PET/CT (18), a normal rest MBF value ranges from 0.4 to 1.2 mL/min/g. The stress MBF value should be higher than 1.7 mL/min/g, and a cutoff of 2.0 for MPR has a higher predictive value for ischemia than the MBF value alone. In studies on quantitative CMR with invasive coronary angiography (ICA) as the reference standard (19,31,35–37), average normal rest MBF values of between 0.8 and 1.3 mL/min/g, average normal stress MBF values of between 2.3 and 3.7 mL/min/g, and average normal MPR values of between 2.6 and 4.1 have been reported (Fig 4). These numbers need to be interpreted within the appropriate clinical context, as normal values for MBF can vary according to the patient's sex, age, and ethnicity. Moreover, an increase in rest MBF can occur due to an increased myocardial workload secondary to increased heart rate or blood pressure caused by a variety of factors (including test-related anxiety, hypertension, etc) in patients with preserved MPR. In such cases, elevated rest MBF may result in low MPR despite normal increased stress MBF. In this scenario, the rest MBF value can be corrected by using the rate-pressure product correction, with the caveat that this correction should be tailored on a case-by-case basis, according to the clinical scenario, by using the following formula:

$$\text{RPP correction} = \frac{\text{Rest MBF}}{\text{SBP} \times \text{HR}} \times \text{RV},$$

where RPP is the rate-pressure product, HR is the heart rate, and RV is a reference value (9000 or 10 000) (18).

## Large-Vessel CAD

The role of stress perfusion CMR in the detection of large-vessel CAD is well established, and this examination has important roles in defining the disease distribution and guiding patient management, including identification of candidates for revascularization. Multiple studies (38,39) have demonstrated the high diagnostic performance of stress CMR, as compared with ICA, in the detection of obstructive CAD, with the advantage of enabling a significantly decreased rate of unnecessary catheterization (2). Stress perfusion CMR and PET, as compared with CT coronary angiography and SPECT, have been shown to have the highest combination of sensitivity and specificity for detection of functionally significant CAD (2).

qPerf CMR studies (19,25,31,35,36) have shown significantly lower stress MBF and MPR in patients with obstructive CAD defined by using ICA, with stress MBF values ranging between 1.4 and 2.5 mL/min/g and MPR values ranging between 1.6 and 2.1 (Fig 5). Stress MBF of 2.01 mL/g/min or lower based on fully automated pixel-wise qPerf can be used to identify

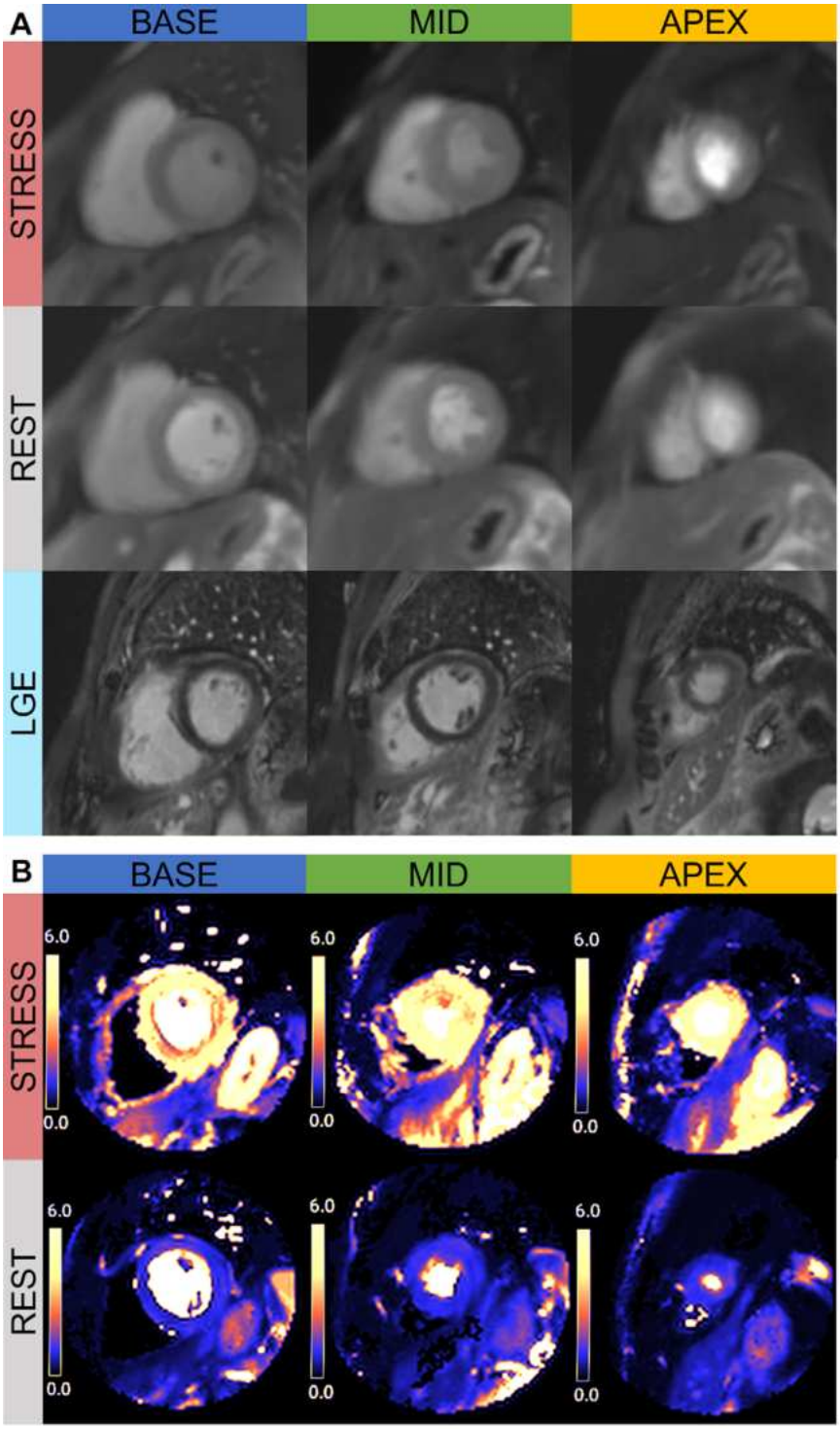


**Figure 4.** **(A)** Stress perfusion CMR image in a 65-year-old woman with chest pain shows no evidence of perfusion defect, and there is no LGE. **(B, C)** Quantification images in this patient show increased stress MBF with high (normal) MPR. Studies on quantitative CMR reported an average normal rest MBF of between 0.8 and 1.3 mL/min/g, an average normal stress MBF of between 2.3 and 3 .7 mL/min/g, and an average normal MPR of between 2.6 and 4.1 (37–39).

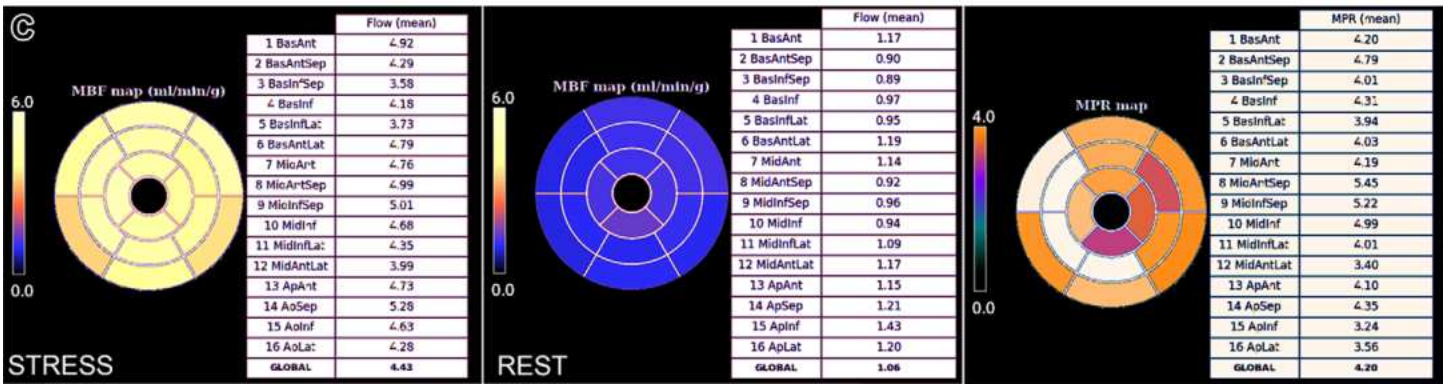

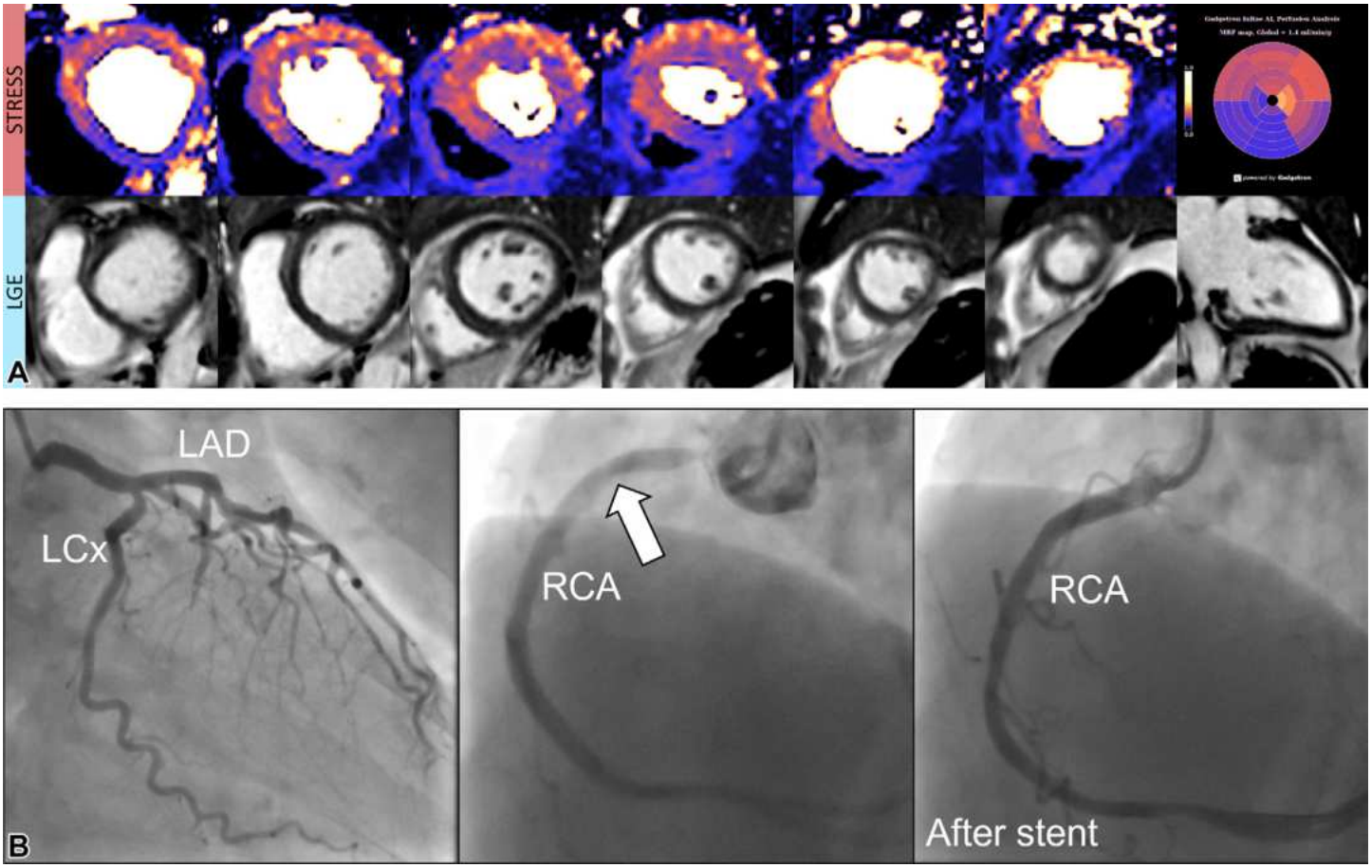


**Figure 5.** **(A)** Quantitative pixel-wise color perfusion maps (top row) and LGE CMR images obtained by using six sections to increase coverage (bottom row) in a 70-year-old woman with chest pain show a perfusion defect in the right coronary artery territory, consistent with inducible ischemia. **(B)** Coronary angiogram findings confirmed the presence of significant stenosis in the right coronary artery *(RCA)* (arrow). A stent was placed. *LAD* = left anterior descending artery, *LCx* = left circumflex artery. (Case courtesy of Henrik Engblom, Lund University Hospital, Lund, Sweden.)

obstructive CAD with high sensitivity (90%) and specificity (89%) (area under receiver operating characteristic curve [AUC], 0.95) (35). In another study, Zhao et al (31) reported that at per-territory analysis, an MPR of 1.86 or lower has the best diagnostic performance in identifying hemodynamically significant CAD (93% sensitivity, 92% specificity [AUC, 0.93]). Fully automated qPerf CMR had higher accuracy in the detection of obstructive CAD (AUC, 0.92) compared with semiquantitative methods (AUC, 0.75–0.82) and qualitative analysis (AUC, 0.70–0.78) (40).

More recent studies (19,31,35,40,41) have confirmed the high diagnostic accuracy of fully automated pixel-wise qPerf CMR and its higher performance compared with that of visual assessment (19,25,42). The most important added value of qPerf imaging is based on its greater capability in distinguishing single-vessel from multivessel disease. In this setting, qualitative assessment is more challenging since a perfusion defect is often more pronounced in one territory and underappreciated in other diseased territories (Fig 6). While the ischemic burden measured with qualitative visual assessment, as compared with quantitative analysis, has been reported to be comparable in patients with nonobstructive or single-vessel disease, in patients with multivessel CAD, the reported ischemic burden measured with qPerf CMR has been significantly higher than that measured with visual assessment: In one study (19), the ischemic burden measured on three-vessel disease maps was 100%, as compared with 56% when it was measured at visual assessment ($P < .001$), and that measured on two-vessel disease maps was 63%, as compared with 41% when it was measured at visual assessment ($P < .001$). In that study (19), the overall accuracy of qPerf mapping for detecting the extent of CAD was significantly higher (78%) than that of visual assessment (58%). These findings show that qPerf CMR significantly enhances the diagnosis of ischemic burden, increasing its prognostic value.

Future directions to improve the diagnostic accuracy of qPerf CMR include increasing myocardial coverage with additional short-axis and/or long-axis planes. Nazir et al (37,43) showed that increasing the spatial coverage to six sections by using simultaneous multislice imaging with iterative reconstruction led to high diagnostic accuracy in detecting obstructive CAD without compromising the temporal resolution, strongly correlating with the conventional three-section technique while improving confidence to diagnose ischemia (Fig 5) (23).

In patients who have acute chest pain and intermediate risk with known CAD, stress CMR can also yield important information for identifying patients who will benefit from revascularization. However, the role of qPerf in this setting has not been explored yet (7).

**Figure 6.** Perfusion defects in a 69-year-old woman with new-onset heart failure (Movie 1). **(A)** Perfusion CMR images show a myocardial perfusion defect (large arrow) in the mid-anterior and septal walls, corresponding to an infarct, as demonstrated by the presence of subendocardial LGE in the same territory. A subtle ischemic perfusion defect (small arrow) in the basal and apical anterior and septal segments is also seen. **(B, C)** Quantification perfusion images **(B)** and MBF and MPR maps **(C)** show globally reduced stress MBF with reduced MPR in all coronary territories, raising concern for multivessel epicardial CAD. **(D)** Left heart catheterization findings confirmed the presence of three-vessel CAD, with total occlusion (large arrow) of the proximal left anterior descending artery *(LAD)* and 70% stenosis (small arrows) of the left circumflex artery *(LCx)* and right coronary artery *(RCA)*.

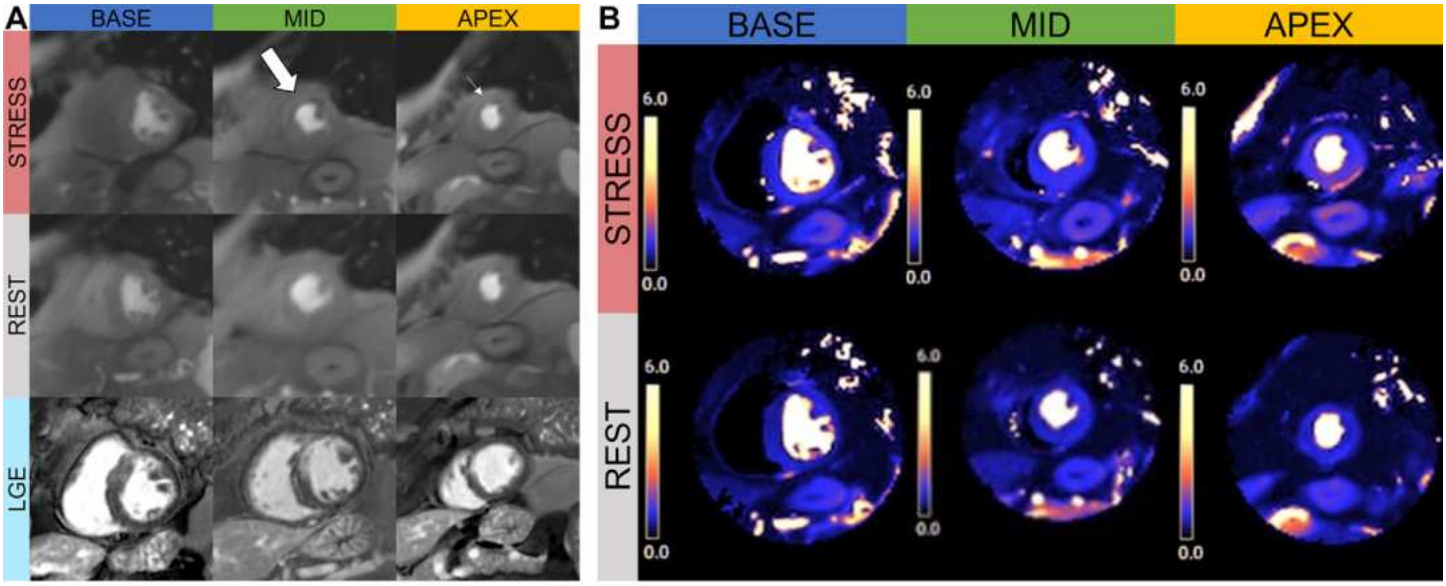


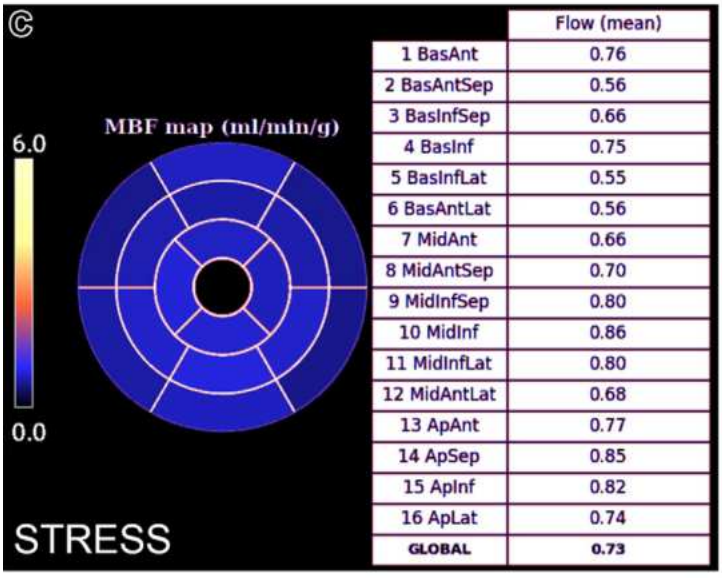


| | Flow (mean) |
|---|---|
| 1 BasAnt | 0.76 |
| 2 BasAntSep | 0.56 |
| 3 BasInfSep | 0.66 |
| 4 BasInf | 0.75 |
| 5 BasInfLat | 0.55 |
| 6 BasAntLat | 0.56 |
| 7 MidAnt | 0.66 |
| 8 MidAntSep | 0.70 |
| 9 MidInfSep | 0.80 |
| 10 MidInf | 0.86 |
| 11 MidInfLat | 0.80 |
| 12 MidAntLat | 0.68 |
| 13 ApAnt | 0.77 |
| 14 ApSep | 0.85 |
| 15 ApInf | 0.82 |
| 16 ApLat | 0.74 |
| GLOBAL | 0.73 |

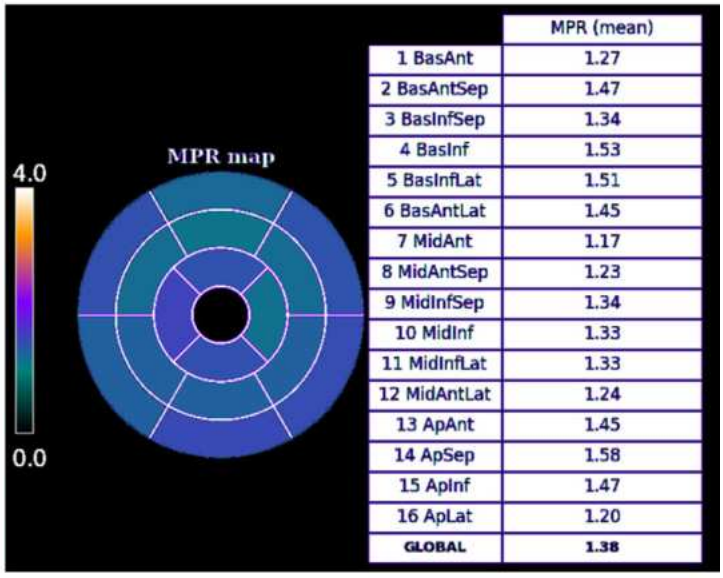


| | MPR (mean) |
|---|---|
| 1 BasAnt | 1.27 |
| 2 BasAntSep | 1.47 |
| 3 BasInfSep | 1.34 |
| 4 BasInf | 1.53 |
| 5 BasInfLat | 1.51 |
| 6 BasAntLat | 1.45 |
| 7 MidAnt | 1.17 |
| 8 MidAntSep | 1.23 |
| 9 MidInfSep | 1.34 |
| 10 MidInf | 1.33 |
| 11 MidInfLat | 1.33 |
| 12 MidAntLat | 1.24 |
| 13 ApAnt | 1.45 |
| 14 ApSep | 1.58 |
| 15 ApInf | 1.47 |
| 16 ApLat | 1.20 |
| GLOBAL | 1.38 |

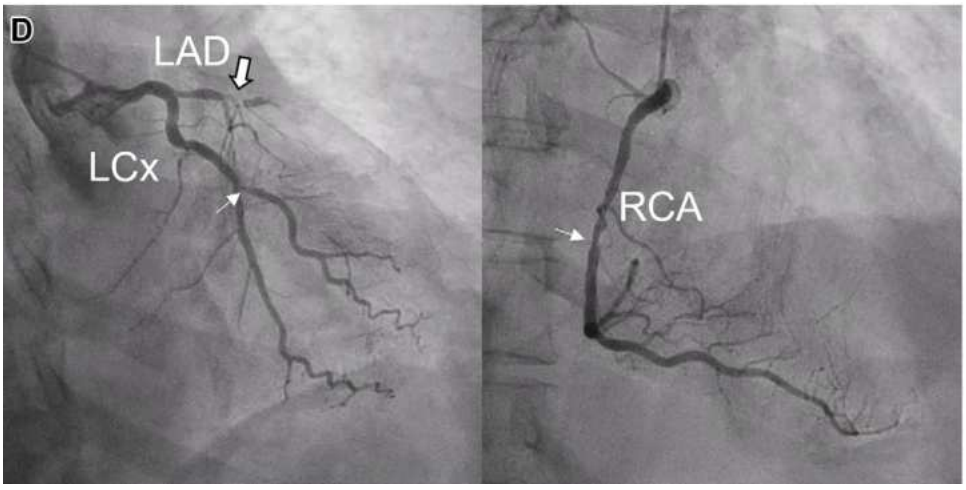

## Microvascular Dysfunction

Coronary MVD or impaired flow reserve within the coronary microvasculature can cause chest pain and ischemia independently of the presence of large-vessel CAD or structural disease (8). MVD was first described as *syndrome X* to identify patients who have ischemia with nonobstructive CAD and is still considered a medical dilemma in terms of pathophysiology, diagnosis, and treatment. Patients who have ischemia with nonobstructive CAD usually have risk factors similar to those in patients with CAD (eg, hypertension, diabetes, smoking, etc). These risk factors are ultimately believed to be responsible for the altered capability of the cardiac microvasculature to regulate MBF (8). Globally reduced stress MBF and MPR in the presence of an adequate hemodynamic response without regional perfusion defects or structural disease suggest MVD (28).

Studies on qPerf CMR have shown significantly lower stress MBF and MPR in patients with MVD defined with use of invasive coronary flow quantification, with stress MBF values ranging between 2.03 and 2.52 mL/min/g and MPR values ranging between 2.2 and 2.4 (Fig 7) (35,44). Rahman et al (45) reported a significantly lower mean MPR (2.00 vs 2.68) and ratio between endocardial and epicardial MPR (MPR ratio, 1.87 vs 2.68) in patients with MVD (defined by invasive coronary flow reserve [CFR] <2.5) compared with those in patients without MVD (CFR ≥2.5) and observed greater diagnostic accuracy with qPerf CMR than with visual assessment to detect MVD. An MPR value of 2.2 and a subendocardial MPR of 2.4 had the highest performance in the detection of MVD. It is interesting that the study from Rahman et al (45) did not show a significant difference in mean stress MBF between the patients with MVD (2.67 mL/min/g) and the patients without MVD (2.99 mL/min/g) ($P = .04$), while the mean rest MBF was significantly higher (1.38 vs 1.14 mL/min/g) in the MVD group ($P < .001$).

Based on these results, stress perfusion CMR with MBF quantification has been introduced into the most recent recommendations for diagnosis in patients who have ischemia, with nonobstructive CAD as the noninvasive diagnostic examination of choice (together with stress PET) for patients with stable chest pain who are suspected of having ischemia with nonobstructive CAD (2a level of evidence). The selection of stress PET versus stress perfusion CMR as the examination of choice should be guided by the local availability of the examination and the level of expertise to perform it (4). Transmural gradients of stress MBF are an important discriminant of MVD and give stress CMR a significant advantage over quantitative PET, which is not cardiac gated and lacks sufficient spatial resolution for transmural flow assessment.

Distinguishing MVD from three-vessel CAD in patients who present with chest pain and are found to have globally reduced MBF and MPR during qPerf CMR is an important diagnostic challenge. Kotecha et al (35) reported a greater reduction in stress MBF and MPR in patients with three-vessel CAD than in those who had MVD. In the Kotecha et al study (35), global stress MBF and MPR values differed significantly among individuals with obstructive CAD, MVD, or normal coronary physiology at ICA and patients in the control groups ($P < .001$). Compared with MBF and MPR values in the patients with normal coronary physiology (global stress MBF, 2.74 mL/g/min; global MPR, 2.59) and in the control subjects (global stress MBF, 3.17 mL/g/min; global MPR, 4.11), the most severe decreases in global stress MBF and MPR were observed in the patients with obstructive three-vessel CAD (global stress MBF, 1.40 mL/g/min; global MPR, 1.71), followed by the patients with MVD, who had moderate decreases in these parameters (global stress MBF, 2.03 mL/g/min; global MPR, 2.37) (35).

Thus, while stress MBF of 2.25 mL/g/min or greater can be used to differentiate normal from abnormal (either obstructive CAD or MVD) blood flow with high accuracy (AUC, 0.96), stress MBF of 1.82 mL/g/min or lower can be used to differentiate obstructive three-vessel CAD from MVD (AUC, 0.99). These results need to be validated in larger studies but demonstrate an important potential future role of qPerf CMR in differentiating these conditions among patients with stable angina (35). qPerf CMR is being used to assess the effectiveness of medical therapies (46) and percutaneous interventions in the setting of microvascular disease (47).

## MVD in Patients with Nonobstructive Cardiomyopathy

### Hypertrophic Cardiomyopathy

HCM is the most common hereditary cardiac disease and has widely variable presentations and prognoses (48). Although some patients may not have symptoms, others may have severe complications such as heart failure, arrhythmia, and sudden cardiac death. Due to the phenotypic heterogeneity of the disease, it is essential to perform risk stratification when managing HCM (48). CMR provides excellent structural and functional information. The identification of LGE, reflecting the presence of myocardial fibrosis, is associated with disease severity and adverse outcomes (49). Patients with HCM may have signs of myocardial ischemia and perfusion abnormalities, even when the coronary arteries are angiographically normal (50). MVD in patients with HCM is attributed to many factors, including arteriole remodeling, dynamic compression of the intramuscular course of the epicardial arteries, inadequate blood supply related to a thickened myocardium, and reduced vasodilator response (51). MVD may have a role in replacement fibrosis, resulting in an adverse prognosis (52).

In one study (53), inducible ischemia was seen at stress perfusion CMR in more than 40% of the patients with HCM and was associated with apical aneurysms, severity of hypertrophy, and nonsustained ventricular tachycardia. Elevated resting flow, predominantly in the endocardium, is an expected finding in patients with HCM due to higher systolic wall tension and increased metabolic requirements (52). Stress MBF and MPR have been significantly decreased in patients with HCM (stress MBF, 1.63 mL/g/min; stress MPR, 2.21) compared with those in control patients (stress MBF, 2.30 mL/g/min; stress MPR, 2.90) and have been correlated with myocardial mass (54). Multiple studies have shown a subendocardial predominance of perfusion defects (51) with an associated transmural gradient between the endocardium and epicardium (52). Perfusion defects have been reported in both the

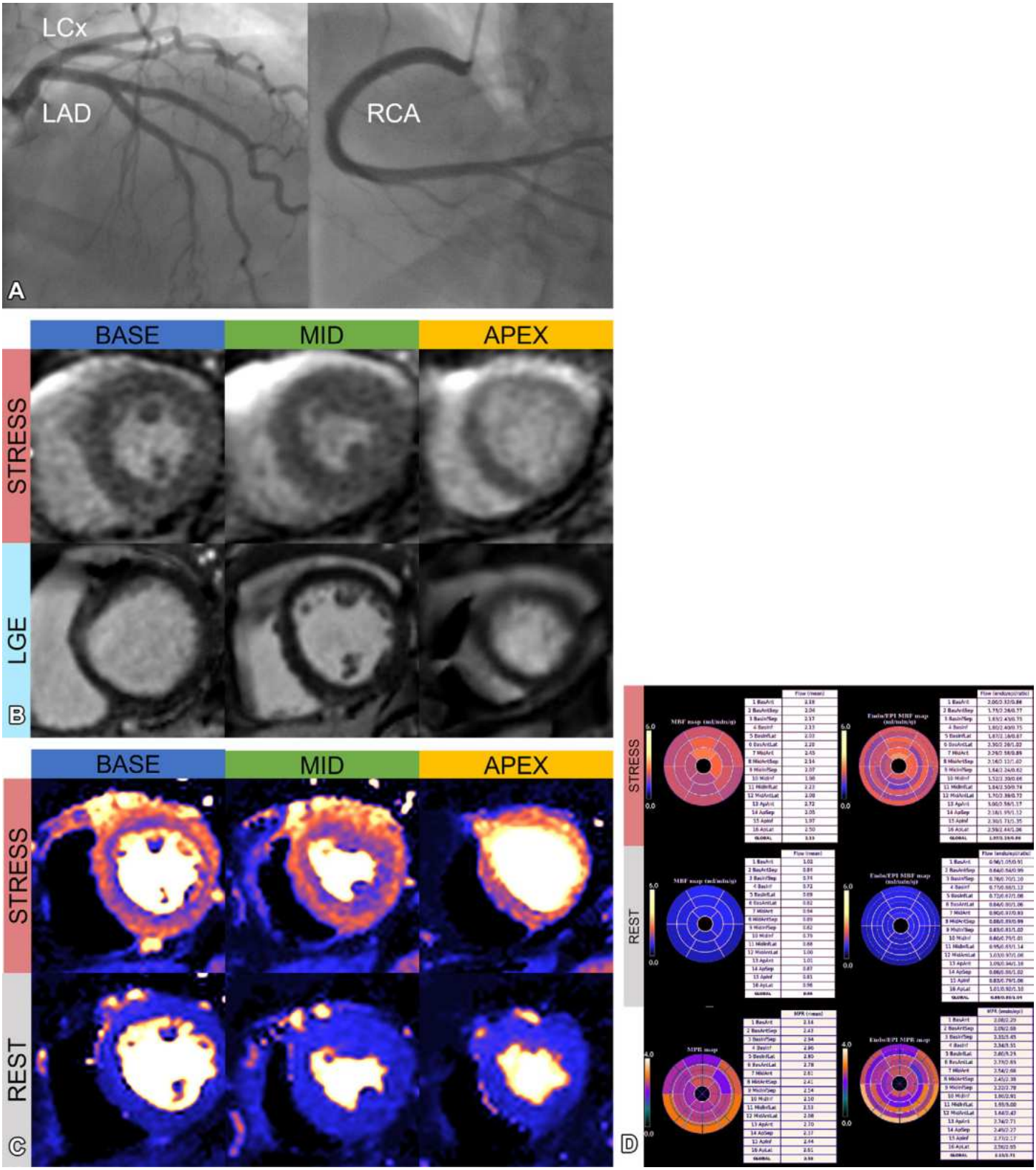


**Figure 7.** Perfusion defect in a 50-year-old woman with diabetes mellitus and hypertension, with progressive exertion-related chest discomfort. **(A)** Invasive coronary angiograms show no obstructive epicardial CAD. *LAD* = left anterior descending artery, *LCx* = left circumflex artery, *RCA* = right coronary artery. **(B, C)** However, stress perfusion images show a reversible perfusion defect that is more prominent at the basal and middle segments and that is not seen at qualitative analysis **(B)** but is evident at quantitative perfusion analysis **(C)**. **(D)** Moreover, perfusion MBF and MPR maps show a transmural gradient across the myocardial wall, with blood flow values lower in the subendocardium than in the epicardium. Findings are consistent with small-vessel ischemia. (Case courtesy of W. Patricia Bandettini, MD, National Institutes of Health, Bethesda, Md.)

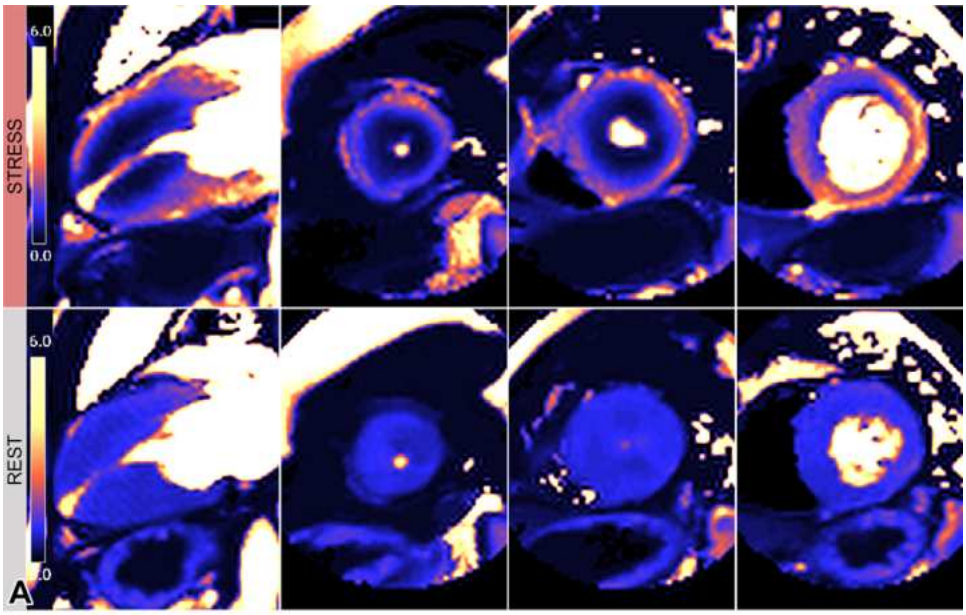


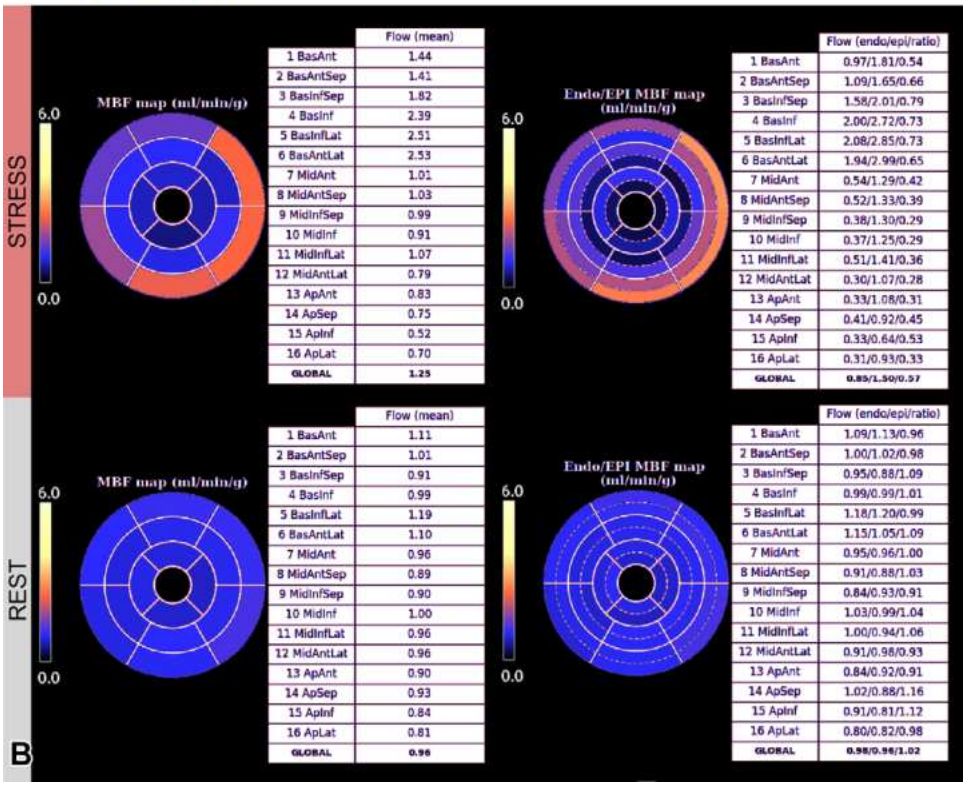


| | Flow (mean) |
|---|---|
| 1 BasAnt | 1.44 |
| 2 BasAntSep | 1.41 |
| 3 BasInfSep | 1.82 |
| 4 BasInf | 2.39 |
| 5 BasInfLat | 2.51 |
| 6 BasAntLat | 2.53 |
| 7 MidAnt | 1.01 |
| 8 MidAntSep | 1.03 |
| 9 MidInfSep | 0.99 |
| 10 MidInf | 0.91 |
| 11 MidInfLat | 1.07 |
| 12 MidAntLat | 0.79 |
| 13 ApAnt | 0.83 |
| 14 ApSep | 0.75 |
| 15 ApInf | 0.52 |
| 16 ApLat | 0.70 |
| GLOBAL | 1.25 |

| | Flow (endo/epi/ratio) |
|---|---|
| 1 BasAnt | 0.97/1.81/0.54 |
| 2 BasAntSep | 1.09/1.65/0.66 |
| 3 BasInfSep | 1.58/2.01/0.79 |
| 4 BasInf | 2.00/2.72/0.73 |
| 5 BasInfLat | 2.08/2.85/0.73 |
| 6 BasAntLat | 1.94/2.99/0.65 |
| 7 MidAnt | 0.54/1.29/0.42 |
| 8 MidAntSep | 0.52/1.33/0.39 |
| 9 MidInfSep | 0.38/1.30/0.29 |
| 10 MidInf | 0.37/1.25/0.29 |
| 11 MidInfLat | 0.51/1.41/0.36 |
| 12 MidAntLat | 0.30/1.07/0.28 |
| 13 ApAnt | 0.33/1.08/0.31 |
| 14 ApSep | 0.41/0.92/0.45 |
| 15 ApInf | 0.33/0.64/0.53 |
| 16 ApLat | 0.31/0.93/0.33 |
| GLOBAL | 0.85/1.50/0.57 |

| | Flow (mean) |
|---|---|
| 1 BasAnt | 1.11 |
| 2 BasAntSep | 1.01 |
| 3 BasInfSep | 0.91 |
| 4 BasInf | 0.99 |
| 5 BasInfLat | 1.19 |
| 6 BasAntLat | 1.10 |
| 7 MidAnt | 0.96 |
| 8 MidAntSep | 0.89 |
| 9 MidInfSep | 0.90 |
| 10 MidInf | 1.00 |
| 11 MidInfLat | 0.96 |
| 12 MidAntLat | 0.96 |
| 13 ApAnt | 0.90 |
| 14 ApSep | 0.93 |
| 15 ApInf | 0.84 |
| 16 ApLat | 0.81 |
| GLOBAL | 0.96 |

| | Flow (endo/epi/ratio) |
|---|---|
| 1 BasAnt | 1.09/1.13/0.96 |
| 2 BasAntSep | 1.00/1.02/0.98 |
| 3 BasInfSep | 0.95/0.88/1.09 |
| 4 BasInf | 0.99/0.99/1.01 |
| 5 BasInfLat | 1.18/1.20/0.99 |
| 6 BasAntLat | 1.15/1.05/1.09 |
| 7 MidAnt | 0.95/0.96/1.00 |
| 8 MidAntSep | 0.91/0.88/1.03 |
| 9 MidInfSep | 0.84/0.93/0.91 |
| 10 MidInf | 1.03/0.99/1.04 |
| 11 MidInfLat | 1.00/0.94/1.06 |
| 12 MidAntLat | 0.91/0.98/0.93 |
| 13 ApAnt | 0.84/0.92/0.91 |
| 14 ApSep | 1.02/0.88/1.16 |
| 15 ApInf | 0.91/0.81/1.12 |
| 16 ApLat | 0.80/0.82/0.98 |
| GLOBAL | 0.98/0.96/1.02 |

**Figure 8.** Hypertrophic cardiomyopathy. qPerf CMR images **(A)** and maps **(B)** show a predominantly subendocardial perfusion defect in the hypertrophied myocardium. (Case courtesy of Konstantinos Moschonas, MBBCh, MRes, MRCP[UK]; and James Moon, MBBCh, FRCP, MD; Barts Heart Center, St Bartholomew's Hospital, London, England.)

hypertrophied myocardium and normal myocardium, and qPerf CMR may be an early assessment tool in HCM gene mutation carriers (Fig 8) (52,55). In a 2021 study (56), 20% of HCM gene mutation carriers were found to have regional perfusion defects at qPerf CMR despite the absence of left ventricle hypertrophy and LGE.

Decreased MPR is associated with the presence of LGE in patients who have HCM. MPR was decreased in patients with HCM, as compared with patients who had mild left ventricle hypertrophy related to aortic stenosis or hypertensive cardiomyopathy (57). In a study by Hughes et al (58), among patients with apical variant HCM, apical perfusion defects were present in 100% of them with both morphologically mild and advanced disease, including those with myocardial fibrosis and apical aneurysms (Fig 9). In such patients, increasing the myocardial coverage to six sections or adding a long-axis plane can be beneficial, enabling better ischemia detection (Fig 10).

## Cardiac Amyloidosis

Cardiac amyloidosis is an infiltrative and restrictive cardiomyopathy characterized by the extracellular deposition of immunoglobulin light chain or transthyretin types of amyloid fibrils. Amyloid proteins accumulate in the extracellular space and may involve all cardiac chambers (59,60). Patients present with symptoms of heart failure, and they also have

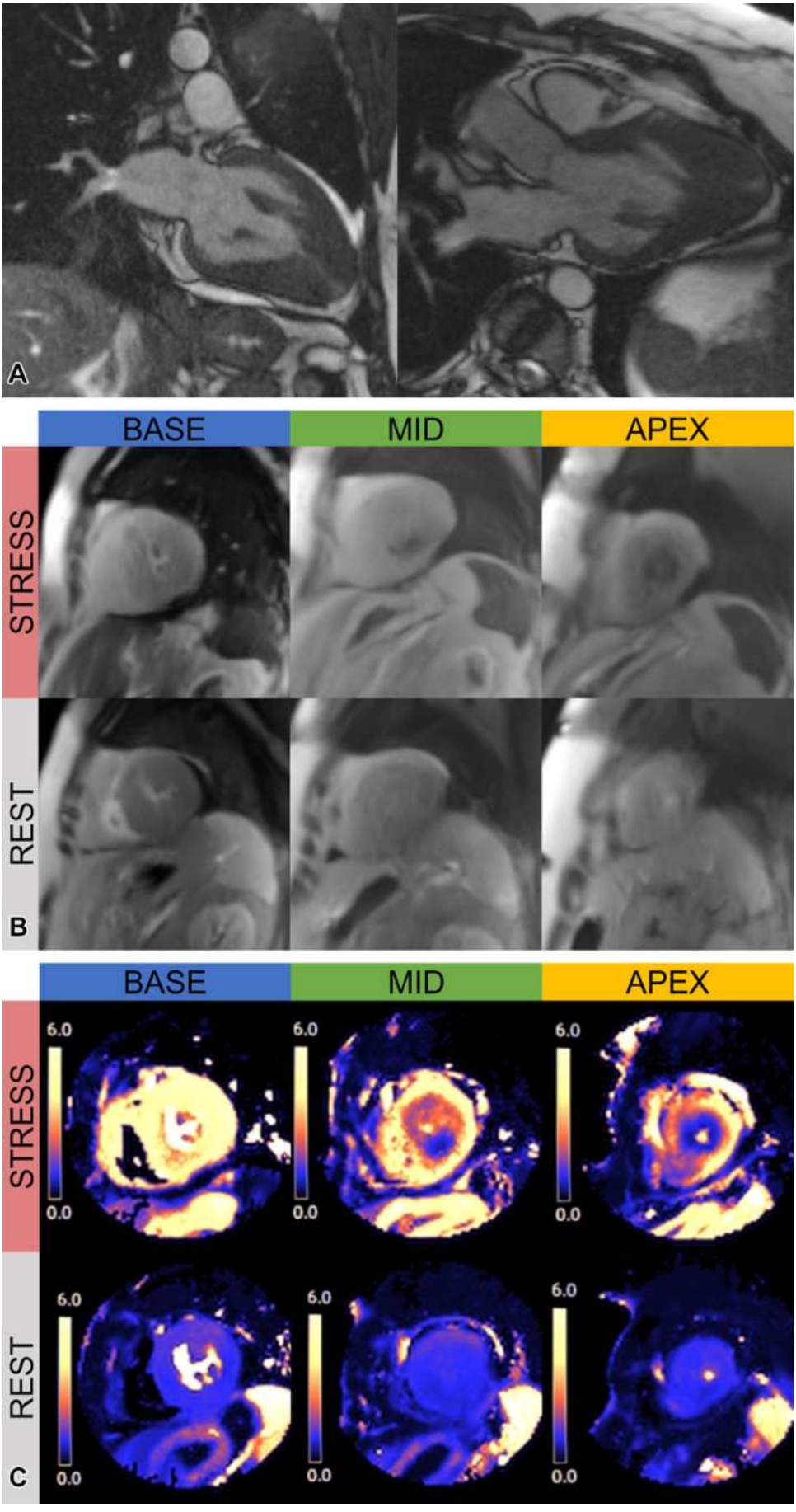


**Figure 9.** Apical variant HCM in a 61-year-old woman with chest pain and no other relevant cardiac history. **(A)** Two-chamber (left) and three-chamber (right) CMR images show hypertrophy of the middle to apical segments, consistent with apical variant HCM. **(B)** Stress perfusion images show a circumferential reversible perfusion defect in the hypertrophic apex and middle wall. **(C)** Quantification perfusion images show reduced MBF at stress and reduced MPR, consistent with MVD in the setting of apical HCM. Stress MBF and MPR were 4.96 mL/g/min and 2.95, respectively, at the base; 1.89 mL/g/min and 1.92, respectively, at the middle segment; and 1.78 mL/g/min and 1.66, respectively, at the apex. Note how quantification analysis revealed a more extensive defect in the middle segment.

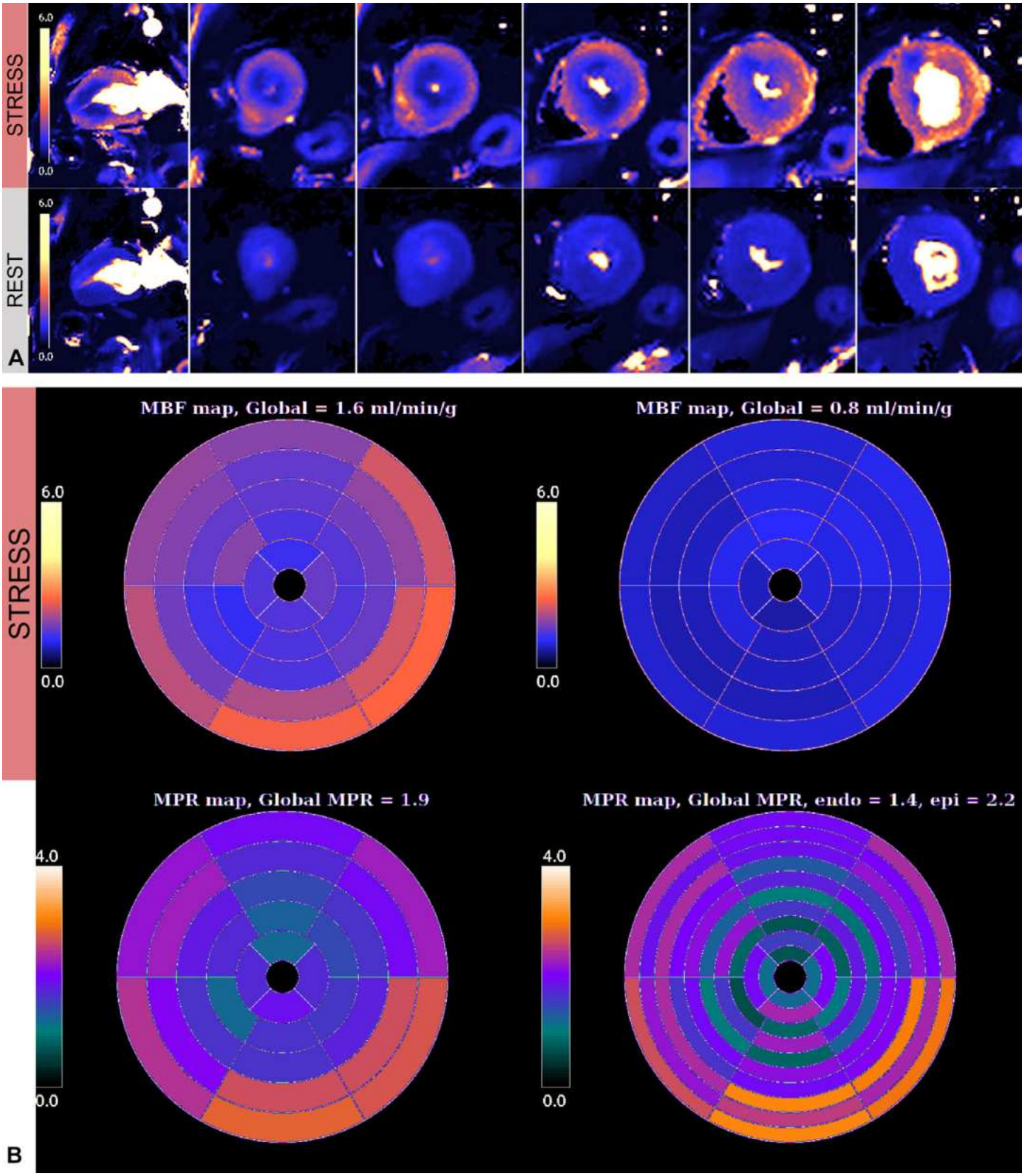


**Figure 10.** Apical variant HCM. Stress perfusion CMR images were obtained with five sections and two-chamber views to increase coverage. **(A)** qPerf CMR images show a reversible perfusion defect in the hypertrophied myocardium and basal septum. **(B)** Stress perfusion maps show significantly reduced MBF and MPR, with significantly decreased MPR in the endocardium. The ratio between the stress MBF and rest MBF was 0.7 (not shown). (Case courtesy of Erik Schelbert, MD, MS, United Hospital, St Paul, Minn.)

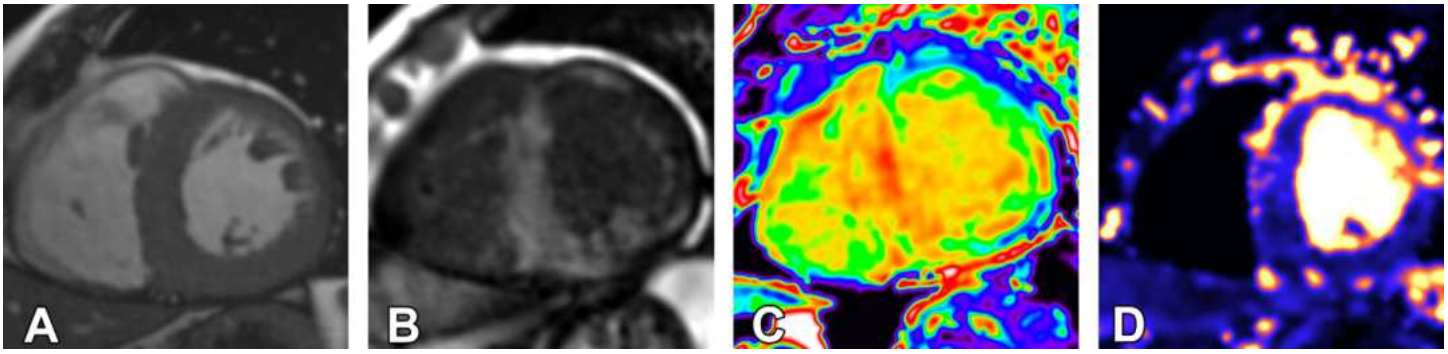


**Figure 11.** Biopsy-proven amyloidosis. Short-axis–view stress perfusion CMR images show concentric left ventricle hypertrophy **(A)** with associated diffuse transmural LGE **(B)**, increased extracellular volume **(C)**, and diffuse decreased stress MBF **(D)**. (Case courtesy of Adam Ioannou, MBBS, BSc, and Marianna Fontana, MD, PhD, National Amyloidosis Center, Royal Free Hospital, London, England.)

angina or a chronically elevated troponin level in the absence of CAD (59). Epicardial arterial and capillary amyloid infiltration results in stenosis of the vessel lumen and capillary disruption, leading to myocardial ischemia and microvascular obstruction (59,61). Although endomyocardial biopsy is the reference standard, CMR is an essential noninvasive diagnostic tool. Difficulty nulling the myocardium on inversion time scout images is highly specific for cardiac amyloidosis. Different patterns of LGE have been described in the literature, with the most common being diffuse subendocardial or transmural enhancement. Elevated native T1 values and extracellular volume also can be diagnostic of cardiac amyloidosis (59,62).

Data on qPerf CMR in the setting of amyloidosis are limited; however, in a recent study, Chacko et al (63) observed significant decreases in stress MBF and MPR (1.04 mL/g/min and 1.57, respectively) in patients with biopsy-proven cardiac amyloidosis compared with those in patients who had angiographically normal coronary arteries (2.92 mL/g/min and 2.78, respectively) and those in healthy volunteers (2.91 mL/g/min and 3.76, respectively). The decrease in stress MBF and MPR in the patients with amyloidosis was comparable to that in the patients with three-vessel disease (stress MBF, 1.35 mL/g/min; stress MPR, 1.54) (Fig 11) (63).

## Cardiac Allograft Vasculopathy

CAV poses a significant challenge in the long-term management of heart allograft recipients and represents a form of chronic rejection characterized by accelerated inflammatory fibroproliferative disease affecting epicardial and/or microvascular coronary arteries. This condition leads to altered myocardial perfusion, chronic ischemic injury, and eventual allograft failure (64). qPerf CMR has emerged as a useful tool for evaluating MBF in heart allograft recipients, with MPR incorporated into the most recent International Society of Heart and Lung Transplant guidelines for CAV detection (class IIb, level C evidence) (65).

The MPR is used to independently predict epicardial and microvascular CAV, having superior diagnostic accuracy for CAV detection compared with ICA in heart allograft recipients over the medium to long term. The MPR can be used to identify severe epicardial or microvascular disease with 79% sensitivity and 85% specificity by using a threshold MPR of 1.65 and to identify moderate epicardial or microvascular disease with 88% sensitivity and 85% specificity by using a threshold MPR of 1.94. MPR has been shown to have greater diagnostic performance than ICA alone (66). Compared with ICA, the MPR can be used to identify CAV (defined as any degree of stenosis at ICA) by using a cutoff value of 1.7 ( with 78% sensitivity and 76% specificity) and to identify severe CAV (defined as >50% stenosis at ICA) by using a cutoff value of 1.4 (with 100% sensitivity and 82% specificity) (67). As in cases of three-vessel CAD, in cases of multivessel involvement, which tends to be more subtle at qualitative analysis, qPerf CMR can be particularly useful (Fig 12).

Resting MBF tends to be higher in heart allograft recipients than in healthy individuals, reflecting the elevated resting rate-pressure product observed after heart transplant. However, stress MBF and MPR are typically lower in the transplant group, indicating compromised perfusion capacity (66).

## Troubleshooting

### Inadequate Vasodilator Response

An inadequate vasodilator response can occur due to multiple factors, most commonly caffeine intake before the examination, despite patients having undergone adequate preparation, as recommended, and having been warned to refrain from using vasodilating agents (eg, caffeine, theophylline, dipyridamole) for 12–24 hours before the examination (14). In addition, older patient age and a reduced ejection fraction can cause an inadequate response to a standard dose of adenosine (68). Absence of a physiologic response (ie, lack of increased heart rate, lack of decreased blood pressure), together with absence of an SSO when adenosine is used, should raise concern for inadequate vasodilator response. As mentioned earlier, SSO is a mechanism that is still not completely understood, and Seitz et al (69) found that it can still occur despite caffeine intake.

qPerf CMR can help to assess for inadequate vasodilator response with decreased stress MBF and MPR (Fig 13). These findings can also mimic myocardial perfusion defects (69). However, in the setting of inadequate response, stress MBF will be nearly identical to rest MBF, with the MPR close to 1.0. Kotecha et al (32) demonstrated that stress MBF greater than 1.43 mL/min/g in at least one segment has the highest accuracy for predicting adequate adenosine response compared with a greater than 10 beats per minute increase in heart rate,

**Figure 12.** Perfusion defect in a 29-year-old man who underwent heart transplant for anthracycline-induced cardiomyopathy in 2007 (Movie 2). **(A)** Myocardial perfusion CMR images show no evidence of a qualitative inducible perfusion defect. **(B, C)** However, quantification perfusion CMR images **(B)** and maps **(C)** show globally reduced stress MBF and MPR in all coronary territories, which are concerning for multivessel coronary involvement in the setting of CAV. **(D)** Left heart catheterization findings confirm the presence of three-vessel disease, showing 80% stenosis of the distal left anterior descending *(LAD)* artery, chronic total occlusion of the middle left circumflex *(LCx)* artery, and 90% stenosis of the distal right coronay artery *(RCA).* Cardiac biopsy results also confirmed the presence of CAV. Note that left heart catheterization performed 2 years previously showed normal coronary arteries in the allograft (not shown), excluding the possibility of CAD secondary to preexisting atherosclerotic disease.

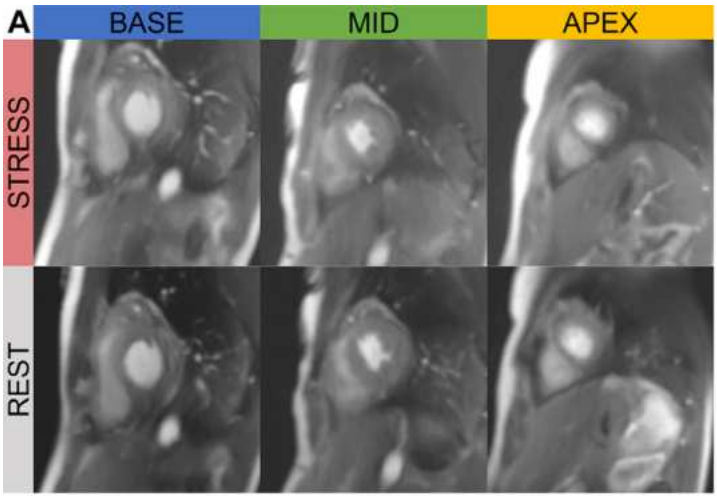


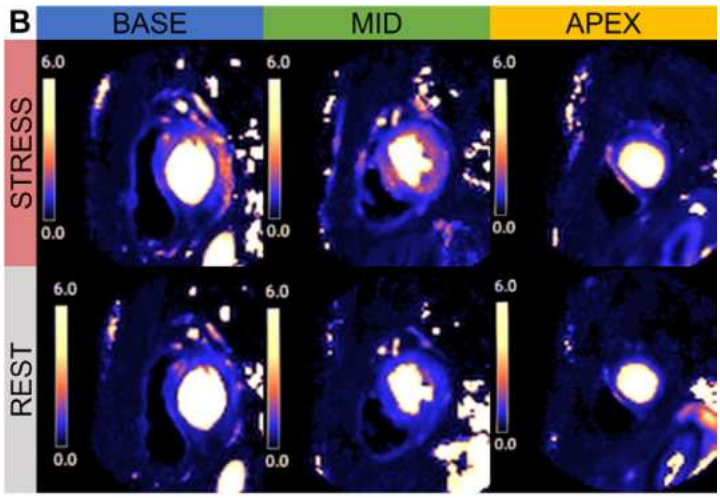


C

MBF map (ml/min/g)

6.0

0.0

STRESS

| | Flow (mean) |
|---|---|
| 1 BasAnt | 1.55 |
| 2 BasAntSep | 1.30 |
| 3 BasInfSep | 1.15 |
| 4 BasInf | 0.72 |
| 5 BasInfLat | 1.35 |
| 6 BasAntLat | 2.05 |
| 7 MidAnt | 1.65 |
| 8 MidAntSep | 1.17 |
| 9 MidInfSep | 1.55 |
| 10 MidInf | 1.50 |
| 11 MidInfLat | 1.53 |
| 12 MidAntLat | 1.35 |
| 13 ApAnt | 1.13 |
| 14 ApSep | 1.07 |
| 15 ApInf | 0.67 |
| 16 ApLat | 0.88 |
| **GLOBAL** | **1.37** |

MPR map

4.0

0.0

| | MPR (mean) |
|---|---|
| 1 BasAnt | 1.43 |
| 2 BasAntSep | 1.15 |
| 3 BasInfSep | 1.29 |
| 4 BasInf | 1.28 |
| 5 BasInfLat | 2.47 |
| 6 BasAntLat | 2.33 |
| 7 MidAnt | 1.67 |
| 8 MidAntSep | 1.29 |
| 9 MidInfSep | 1.58 |
| 10 MidInf | 1.73 |
| 11 MidInfLat | 1.48 |
| 12 MidAntLat | 1.48 |
| 13 ApAnt | 1.70 |
| 14 ApSep | 1.19 |
| 15 ApInf | 1.05 |
| 16 ApLat | 1.27 |
| **GLOBAL** | **1.58** |

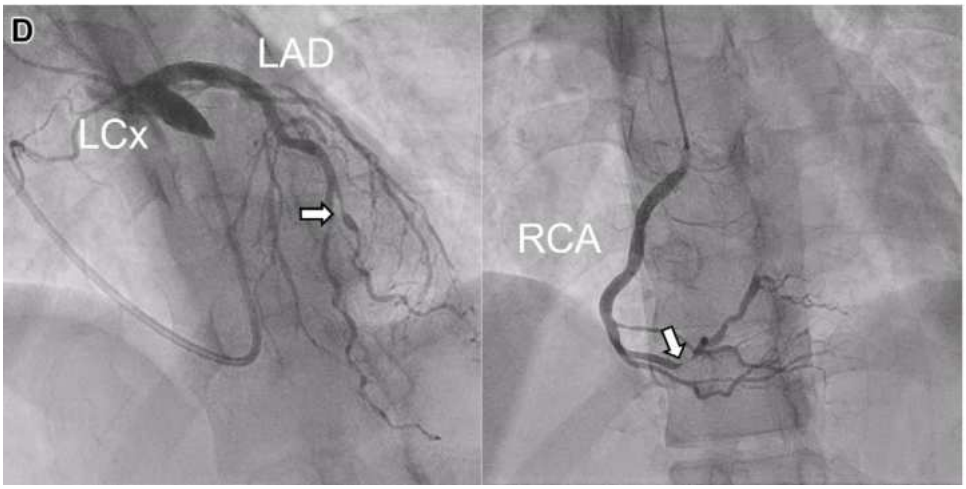

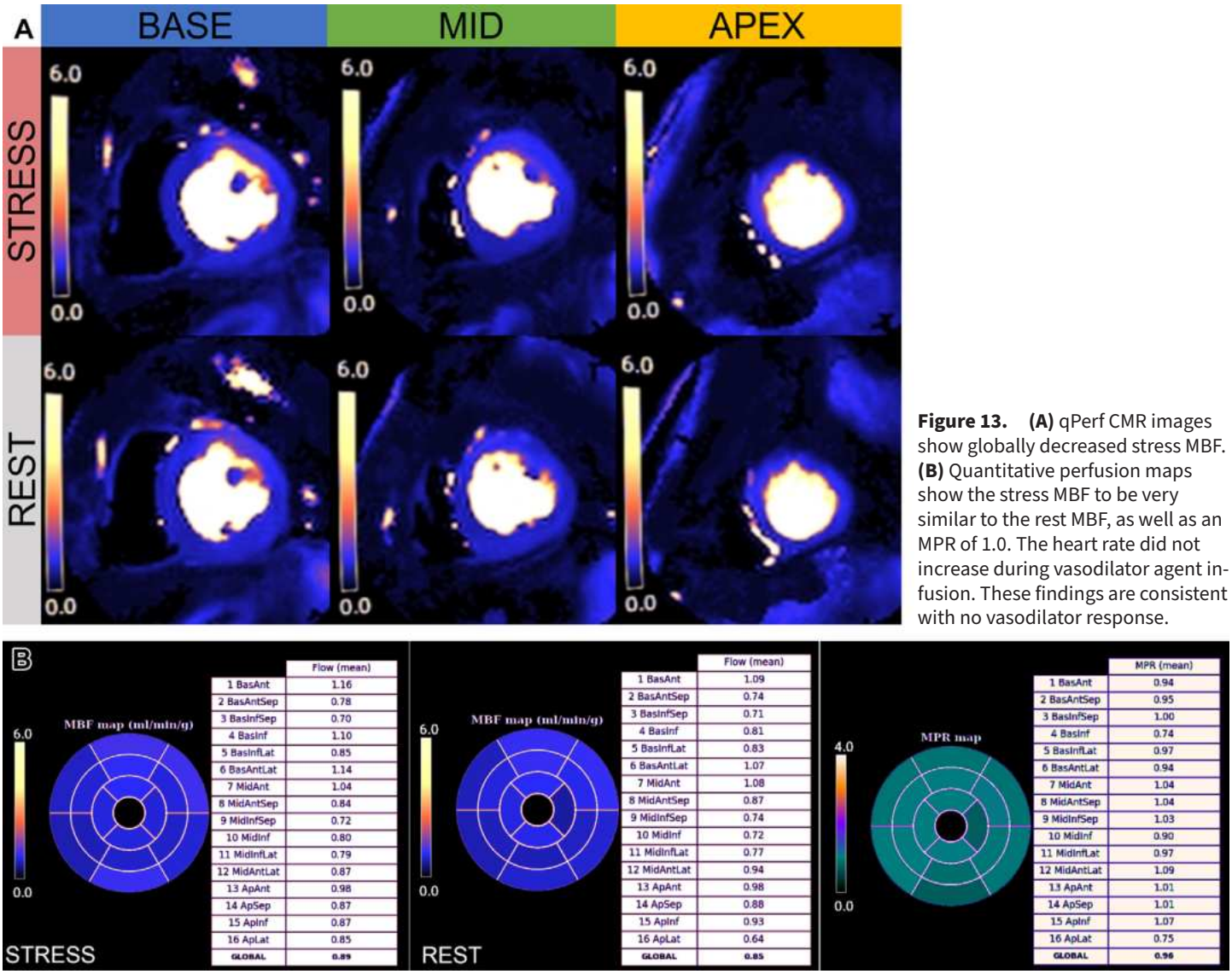


**Figure 13.** **(A)** qPerf CMR images show globally decreased stress MBF. **(B)** Quantitative perfusion maps show the stress MBF to be very similar to the rest MBF, as well as an MPR of 1.0. The heart rate did not increase during vasodilator agent infusion. These findings are consistent with no vasodilator response.

a greater than 10-mm Hg decrease in SBP, and the presence of SSO. Consequently, based on the algorithm proposed by Kotecha et al (32), stress MBF of 1.43 mL/min/g or lower without evidence of a perfusion defect should raise concern for inadequate response. At the time of adenosine administration, if an inadequate response is suspected with a standard adenosine dose (140 mcg/kg/min), the dose can be safely increased to 210 mcg/kg/min (68), particularly in patients with impaired left ventricular systolic function (32).

### Dark Rim Artifact

Dark rim artifact, defined as a subendocardial region of hypointensity that is visible at both stress and rest without associated delayed enhancement on LGE images, is a source of false-positive examinations. Compared with a true reversible perfusion defect, dark rim artifact is most prominent when the contrast material arrives in the left ventricle blood pool, persists only transiently before peak myocardial contrast enhancement, and is approximately one pixel wide (34). In this setting, quantification can help differentiate the artifact from a true myocardial perfusion defect, because in the case of dark rim artifact, quantification will be normal (Fig 14) (70). The occurrence of dark rim artifact can be minimized by using parallel imaging techniques that improve spatial and temporal resolution such as k-t sensitivity-encoded acceleration (k-t SENSE), k-t broad-use liner acquisition speed-up (BLAST), and k-t generalized auto-calibrating partially parallel acquisition (GRAPPA) techniques (71,72).

## Conclusion

qPerf CMR is an emerging and powerful clinical tool that can improve the diagnostic accuracy of stress perfusion CMR in the assessment of ischemia in the setting of epicardial CAD and the noninvasive assessment of MVD and CAV. This examination can also provide insights into the impact of nonobstructive cardiomyopathies on coronary artery pathophysiology. Numerous MRI pulse sequences and software packages for performing qPerf CMR and analyzing qPerf CMR findings are currently available and have expanded the accessibility of this technique to an increasing number of patients and clinicians. As data demonstrating the superior performance of qPerf CMR continue to grow, qPerf CMR will

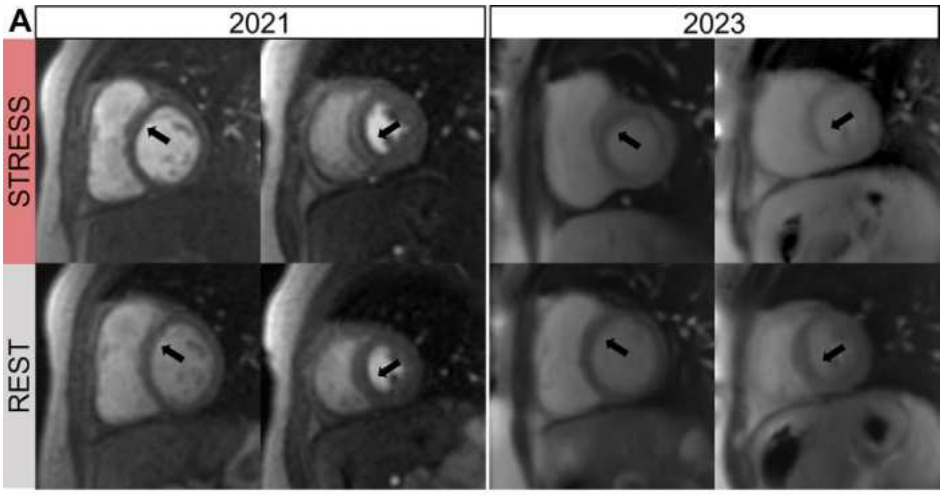


**Figure 14.** Cardiac perfusion surveillance in a 30-year-old woman after heart transplant. **(A)** Stress perfusion CMR images obtained in 2021 show circumferential hypointensity at the base to middle of the septum that is more pronounced at stress than at rest (arrows) and thus concerning for perfusion defect (Movie 3). Subsequent cardiac MR images obtained in 2023 show similar findings (arrows) (Movie 4). **(B)** However, quantification perfusion MR images obtained in 2023 show high MBF at stress with preserved MPR. Findings are consistent with dark rim artifact.

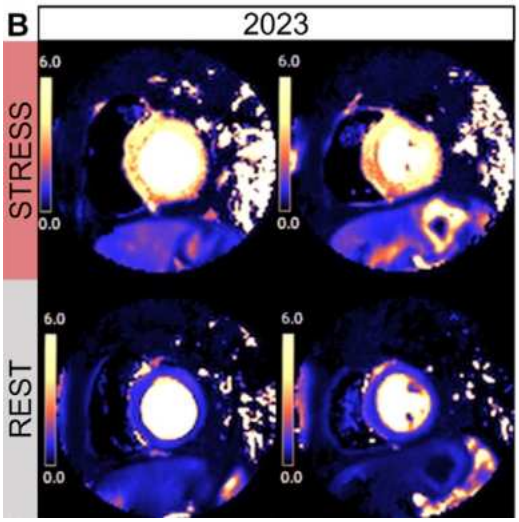


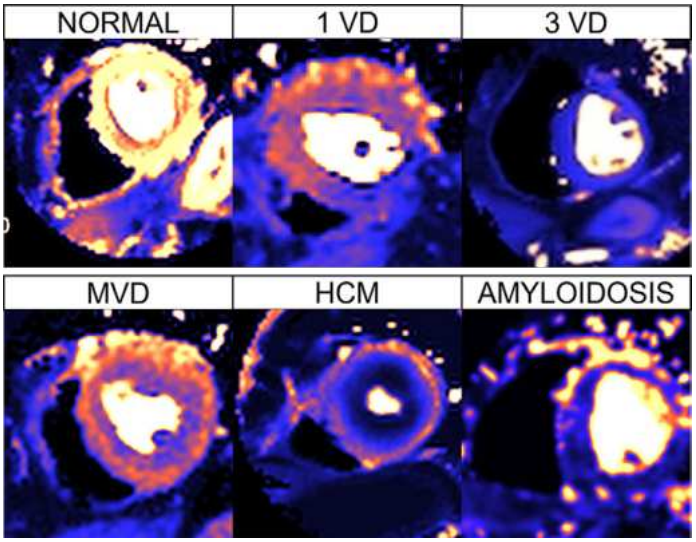


**Figure 15.** Perfusion CMR images depict normal myocardial function, as well as the most relevant causes of ischemia: amyloidosis (case courtesy of Adam Ioannou, MBBS, BSc, and Marianna Fontana, MD, PhD, National Amyloidosis Center, Royal Free Hospital, London, England), HCM (case courtesy of Erik Schelbert, MD, MS, United Hospital, St Paul, Minn), one-vessel disease *(1 VD)* (case courtesy of Henrik Engblom, Lund University Hospital, Lund, Sweden), three-vessel disease *(3 VD),* and MVD (case courtesy of W. Patricia Bandettini, MD, National Institutes of Health, Bethesda, Md.)

probably become a standard tool in the evaluation of CAD. The normal and pathologic conditions seen at qPerf CMR and discussed in this article are summarized in Figure 15. Given the relative novelty of qPerf CMR, additional studies in larger cohorts and across a broad spectrum of diseases such as hypertensive heart disease, severe aortic stenosis (73), dilated cardiomyopathy (74), and systemic sclerosis (75) can be used to further define the role of this examination in clinical practice.

***Author affiliations.***—From the Department of Radiology (R.C., S.Q., A.A.R., T.A.T., J.B.B., K.C., R.A., B.D.A.) and Department of Medicine, Division of Cardiology (D.C.L.), Northwestern University Feinberg School of Medicine, 676 N St. Clair St, Ste 800, Arkes Family Pavilion, Chicago, IL 60611; Cardiovascular MR R&D, Siemens Medical Solutions, Chicago, Ill (K.C.); and National Heart, Lung and Blood Institute, National Institutes of Health, Bethesda, Md (P.K.). Recipient of a Magna Cum Laude award for an education exhibit at the 2023 RSNA Annual Meeting. Received April 15, 2024; revision requested June 12 and received July 23; accepted July 26. **Address correspondence to** R.C. (email: *roberta.catania@northwestern.edu*).

***Acknowledgments.***—The authors would like to acknowledge the contributions of images provided by W. Patricia Bandettini, MD, National Institutes of Health, Bethesda, Md; Henrik Engblom, Lund University Hospital, Lund, Sweden; Erik Schelbert, MD, MS, United Hospital, St Paul, Minn; Konstantinos Moschonas, MBBCh, MRes, MRCP(UK), and James Moon, MBBCh, FRCP, MD, Barts Heart Center, St Bartholomew's Hospital, London, England; and Adam Ioannou, MBBS, BSc, and Marianna Fontana, MD, PhD, National Amyloidosis Center, Royal Free Hospital, London, England.

***Disclosures of conflicts of interest.*—K.C.** Stockholder and full-time employee of Siemens Healthineers. **D.C.L.** Research grants paid to author's institution from Abbott Laboratories; American Heart Association; National Institutes of Health (NIH)/National Heart, Lung, and Blood Institute; and Radiological Society of North America. **R.A.** Consulting fee and honorarium payments from Siemens Healthineers. **B.D.A.** Research support from the NIH, American Heart Association, Guerbet, and Northwestern University; consulting fee payments from Circle Cardiovascular Imaging; payment or honoraria from MRI Online and Circle Cardiovascular Imaging; payment for expert testimony from the U.S. Department of Justice; travel support from Siemens Healthineers; participant on a Data Safety Monitoring Board or Advisory Board of the U.S. Department of Justice; one U.S. patent pending and one U.S. provisional patent with Northwestern University; stockholder and founder of Third Coast Dynamics.

## References

1. Greenwood JP, Maredia N, Younger JF, et al. Cardiovascular magnetic resonance and single-photon emission computed tomography for diagnosis of coronary heart disease (CE-MARC): a prospective trial. Lancet 2012;379(9814):453–460.

2. Knuuti J, Ballo H, Juarez-Orozco LE, et al. The performance of non-invasive tests to rule-in and rule-out significant coronary artery stenosis in patients with stable angina: a meta-analysis focused on post-test disease probability. Eur Heart J 2018;39(35):3322–3330.
3. Nagel E, Greenwood JP, McCann GP, et al; MR-INFORM Investigators. Magnetic Resonance Perfusion or Fractional Flow Reserve in Coronary Disease. N Engl J Med 2019;380(25):2418–2428.
4. Gulati M, Levy PD, Mukherjee D, et al. 2021 AHA/ACC/ASE/CHEST/SAEM/SCCT/SCMR Guideline for the Evaluation and Diagnosis of Chest Pain: A Report of the American College of Cardiology/American Heart Association Joint Committee on Clinical Practice Guidelines. Circulation 2021;144(22):e368–e454. [Published corrections appear in Circulation 2021;144(22):e455 and Circulation 2023;148(24):e281.]
5. Goodwill AG, Dick GM, Kiel AM, Tune JD. Regulation of Coronary Blood Flow. Compr Physiol 2017;7(2):321–382.
6. Villa AD, Sammut E, Nair A, Rajani R, Bonamini R, Chiribiri A. Coronary artery anomalies overview: the normal and the abnormal. World J Radiol 2016;8(6):537–555.
7. Duncker DJ, Koller A, Merkus D, Canty JM Jr. Regulation of coronary blood flow in health and ischemic heart disease. Prog Cardiovasc Dis 2015;57(5):409–422.
8. Camici PG, d'Amati G, Rimoldi O. Coronary microvascular dysfunction: mechanisms and functional assessment. Nat Rev Cardiol 2015;12(1):48–62.
9. Merkus D, Muller-Delp J, Heaps CL. Coronary microvascular adaptations distal to epicardial artery stenosis. Am J Physiol Heart Circ Physiol 2021;320(6):H2351–H2370.
10. Botvinick EH. Current methods of pharmacologic stress testing and the potential advantages of new agents. J Nucl Med Technol 2009;37(1):14–25.
11. Bastarrika G, Ezponda A, Baizan AG, et al. Safety of regadenoson for vasodilation in cardiac MRI stress tests [in Spanish]. Radiologia (Engl Ed) 2020;62(3):213–221. https://doi.org/10.1016/j.rxeng.2020.01.002.
12. Bhave NM, Freed BH, Yodwut C, et al. Considerations when measuring myocardial perfusion reserve by cardiovascular magnetic resonance using regadenoson. J Cardiovasc Magn Reson 2012;14(1):89.
13. Le TT, Huang W, Bryant JA, Cook SA, Chin CW. Stress cardiovascular magnetic resonance imaging: current and future perspectives. Expert Rev Cardiovasc Ther 2017;15(3):181–189.
14. Kramer CM, Barkhausen J, Bucciarelli-Ducci C, Flamm SD, Kim RJ, Nagel E. Standardized cardiovascular magnetic resonance imaging (CMR) protocols: 2020 update. J Cardiovasc Magn Reson 2020;22(1):17.
15. Gebhard C, Messerli M, Lohmann C, et al. Sex and age differences in the association of heart rate responses to adenosine and myocardial ischemia in patients undergoing myocardial perfusion imaging. J Nucl Cardiol 2020;27(1):159–170.
16. Patriki D, von Felten E, Bakula A, et al. Splenic switch-off as a predictor for coronary adenosine response: validation against 13N-ammonia during co-injection myocardial perfusion imaging on a hybrid PET/CMR scanner. J Cardiovasc Magn Reson 2021;23(1):3.
17. Zhou W, Sin J, Yan AT, et al. Qualitative and Quantitative Stress Perfusion Cardiac Magnetic Resonance in Clinical Practice: A Comprehensive Review. Diagnostics (Basel) 2023;13(3):13.
18. Bateman TM, Heller GV, Beanlands R, et al. Practical Guide for Interpreting and Reporting Cardiac PET Measurements of Myocardial Blood Flow: An Information Statement from the American Society of Nuclear Cardiology, and the Society of Nuclear Medicine and Molecular Imaging. J Nucl Med 2021;62(11):1599–1615.
19. Kotecha T, Chacko L, Chehab O, et al. Assessment of Multivessel Coronary Artery Disease Using Cardiovascular Magnetic Resonance Pixelwise Quantitative Perfusion Mapping. JACC Cardiovasc Imaging 2020;13(12):2546–2557.
20. Thomas KE, Fotaki A, Botnar RM, Ferreira VM. Imaging Methods: Magnetic Resonance Imaging. Circ Cardiovasc Imaging 2023;16(1):e014068.
21. Fraum TJ, Ludwig DR, Bashir MR, Fowler KJ. Gadolinium-based contrast agents: a comprehensive risk assessment. J Magn Reson Imaging 2017;46(2):338–353.
22. Raman SV, Markl M, Patel AR, et al. 30-minute CMR for common clinical indications: a Society for Cardiovascular Magnetic Resonance white paper. J Cardiovasc Magn Reson 2022;24(1):13.
23. Engblom H, Ostenfeld E, Carlsson M, et al. Diagnostic confidence with quantitative cardiovascular magnetic resonance perfusion mapping increases with increased coverage of the left ventricle. J Cardiovasc Magn Reson 2024;26(1):101007.
24. Min JY, Ko SM, Song IY, Yi JG, Hwang HK, Shin JK. Comparison of the Diagnostic Accuracies of 1.5T and 3T Stress Myocardial Perfusion Cardiovascular Magnetic Resonance for Detecting Significant Coronary Artery Disease. Korean J Radiol 2018;19(6):1007–1020.
25. Lockie T, Ishida M, Perera D, et al. High-resolution magnetic resonance myocardial perfusion imaging at 3.0-Tesla to detect hemodynamically significant coronary stenoses as determined by fractional flow reserve. J Am Coll Cardiol 2011;57(1):70–75.
26. Yun CH, Tsai JP, Tsai CT, et al. Qualitative and semi-quantitative evaluation of myocardium perfusion with 3 T stress cardiac MRI. BMC Cardiovasc Disord 2015;15(1):164.
27. Kellman P, Hansen MS, Nielles-Vallespin S, et al. Myocardial perfusion cardiovascular magnetic resonance: optimized dual sequence and reconstruction for quantification. J Cardiovasc Magn Reson 2017;19(1):43.
28. Sharrack N, Chiribiri A, Schwitter J, Plein S. How to do quantitative myocardial perfusion cardiovascular magnetic resonance. Eur Heart J Cardiovasc Imaging 2022;23(3):315–318.
29. Attili AK, Schuster A, Nagel E, Reiber JH, van der Geest RJ. Quantification in cardiac MRI: advances in image acquisition and processing. Int J Cardiovasc Imaging 2010;26(Suppl 1):27–40.
30. Engblom H, Xue H, Akil S, et al. Fully quantitative cardiovascular magnetic resonance myocardial perfusion ready for clinical use: a comparison between cardiovascular magnetic resonance imaging and positron emission tomography. J Cardiovasc Magn Reson 2017;19(1):78.
31. Zhao SH, Guo WF, Yao ZF, et al. Fully automated pixel-wise quantitative CMR-myocardial perfusion with CMR-coronary angiography to detect hemodynamically significant coronary artery disease. Eur Radiol 2023;33(10):7238–7249.
32. Kotecha T, Monteagudo JM, Martinez-Naharro A, et al. Quantitative cardiovascular magnetic resonance myocardial perfusion mapping to assess hyperaemic response to adenosine stress. Eur Heart J Cardiovasc Imaging 2021;22(3):273–281.
33. Klem I, Heitner JF, Shah DJ, et al. Improved detection of coronary artery disease by stress perfusion cardiovascular magnetic resonance with the use of delayed enhancement infarction imaging. J Am Coll Cardiol 2006;47(8):1630–1638.
34. Schulz-Menger J, Bluemke DA, Bremerich J, et al. Standardized image interpretation and post-processing in cardiovascular magnetic resonance: 2020 update—Society for Cardiovascular Magnetic Resonance (SCMR): Board of Trustees Task Force on Standardized Post-Processing. J Cardiovasc Magn Reson 2020;22(1):19.
35. Kotecha T, Martinez-Naharro A, Boldrini M, et al. Automated Pixel-Wise Quantitative Myocardial Perfusion Mapping by CMR to Detect Obstructive Coronary Artery Disease and Coronary Microvascular Dysfunction: Validation Against Invasive Coronary Physiology. JACC Cardiovasc Imaging 2019;12(10):1958–1969.
36. Motwani M, Kidambi A, Sourbron S, et al. Quantitative three-dimensional cardiovascular magnetic resonance myocardial perfusion imaging in systole and diastole. J Cardiovasc Magn Reson 2014;16(1):19.
37. Nazir MS, Milidonis X, McElroy S, et al. Quantitative Myocardial Perfusion With Simultaneous-Multislice Stress CMR for Detection of Significant Coronary Artery Disease. JACC Cardiovasc Imaging 2022;15(9):1672–1674.
38. Jiang B, Cai W, Lv X, Liu H. Diagnostic Performance and Clinical Utility of Myocardial Perfusion MRI for Coronary Artery Disease with Fractional Flow Reserve as the Standard Reference: A Meta-analysis. Heart Lung Circ 2016;25(10):1031–1038.
39. Li M, Zhou T, Yang LF, Peng ZH, Ding J, Sun G. Diagnostic accuracy of myocardial magnetic resonance perfusion to diagnose ischemic stenosis with fractional flow reserve as reference: systematic review and meta-analysis. JACC Cardiovasc Imaging 2014;7(11):1098–1105.
40. Mordini FE, Haddad T, Hsu LY, et al. Diagnostic accuracy of stress perfusion CMR in comparison with quantitative coronary angiography: fully quantitative, semiquantitative, and qualitative assessment. JACC Cardiovasc Imaging 2014;7(1):14–22.
41. Hsu LY, Jacobs M, Benovoy M, et al. Diagnostic Performance of Fully Automated Pixel-Wise Quantitative Myocardial Perfusion Imaging by Cardiovascular Magnetic Resonance. JACC Cardiovasc Imaging 2018;11(5):697–707.
42. Patel AR, Antkowiak PF, Nandalur KR, et al. Assessment of advanced coronary artery disease: advantages of quantitative cardiac magnetic resonance perfusion analysis. J Am Coll Cardiol 2010;56(7):561–569.
43. Nazir MS, Neji R, Speier P, et al. Simultaneous multi slice (SMS) balanced steady state free precession first-pass myocardial perfusion cardiovascular magnetic resonance with iterative reconstruction at 1.5 T. J Cardiovasc Magn Reson 2018;20(1):84.
44. Zorach B, Shaw PW, Bourque J, et al. Quantitative cardiovascular magnetic resonance perfusion imaging identifies reduced flow reserve in microvascular coronary artery disease. J Cardiovasc Magn Reson 2018;20(1):14.
45. Rahman H, Scannell CM, Demir OM, et al. High-Resolution Cardiac Magnetic Resonance Imaging Techniques for the Identification of Coronary Microvascular Dysfunction. JACC Cardiovasc Imaging 2021;14(5):978–986.

46. Morrow AJ, Ford TJ, Mangion K, et al. Rationale and design of the Medical Research Council's Precision Medicine with Zibotentan in Microvascular Angina (PRIZE) trial. Am Heart J 2020;229:70–80.
47. Foley MJ, Rajkumar CA, Ahmed-Jushuf F, et al. Coronary sinus reducer for the treatment of refractory angina (ORBITA-COSMIC): a randomised, placebo-controlled trial. Lancet 2024;403(10436):1543–1553.
48. Maron BJ. Hypertrophic cardiomyopathy: a systematic review. JAMA 2002;287(10):1308–1320.
49. Weng Z, Yao J, Chan RH, et al. Prognostic Value of LGE-CMR in HCM: A Meta-Analysis. JACC Cardiovasc Imaging 2016;9(12):1392–1402.
50. Camici PG, Crea F. Coronary microvascular dysfunction. N Engl J Med 2007;356(8):830–840.
51. Tyan CC, Armstrong S, Scholl D, et al. Stress hypoperfusion and tissue injury in hypertrophic cardiomyopathy: spatial characterization using high-resolution 3-tesla magnetic resonance imaging. Circ Cardiovasc Imaging 2013;6(2):229–238.
52. Ismail TF, Hsu LY, Greve AM, et al. Coronary microvascular ischemia in hypertrophic cardiomyopathy: a pixel-wise quantitative cardiovascular magnetic resonance perfusion study. J Cardiovasc Magn Reson 2014;16(1):49.
53. Kim EK, Lee SC, Chang SA, et al. Prevalence and clinical significance of cardiovascular magnetic resonance adenosine stress-induced myocardial perfusion defect in hypertrophic cardiomyopathy. J Cardiovasc Magn Reson 2020;22(1):30.
54. Camaioni C, Knott KD, Augusto JB, et al. Inline perfusion mapping provides insights into the disease mechanism in hypertrophic cardiomyopathy. Heart 2020;106(11):824–829.
55. Garcia Brás P, Aguiar Rosa S, Thomas B, et al. Associations between perfusion defects, tissue changes and myocardial deformation in hypertrophic cardiomyopathy, uncovered by a cardiac magnetic resonance segmental analysis. Rev Port Cardiol 2022;41(7):559–568.
56. Hughes RK, Camaioni C, Augusto JB, et al. Myocardial Perfusion Defects in Hypertrophic Cardiomyopathy Mutation Carriers. J Am Heart Assoc 2021;10(15):e020227.
57. Tezuka D, Kosuge H, Terashima M, et al. Myocardial perfusion reserve quantified by cardiac magnetic resonance imaging is associated with late gadolinium enhancement in hypertrophic cardiomyopathy. Heart Vessels 2018;33(5):513–520.
58. Hughes RK, Augusto JB, Knott K, et al. Apical Ischemia Is a Universal Feature of Apical Hypertrophic Cardiomyopathy. Circ Cardiovasc Imaging 2023;16(3):e014907.
59. Dorbala S, Cuddy S, Falk RH. How to Image Cardiac Amyloidosis: A Practical Approach. JACC Cardiovasc Imaging 2020;13(6):1368–1383.
60. Razvi Y, Patel RK, Fontana M, Gillmore JD. Cardiac Amyloidosis: A Review of Current Imaging Techniques. Front Cardiovasc Med 2021;8:751293.
61. Dorbala S, Vangala D, Bruyere J Jr, et al. Coronary microvascular dysfunction is related to abnormalities in myocardial structure and function in cardiac amyloidosis. JACC Heart Fail 2014;2(4):358–367.
62. Dorbala S, Ando Y, Bokhari S, et al. ASNC/AHA/ASE/EANM/HFSA/ISA/SCMR/SNMMI Expert Consensus Recommendations for Multimodality Imaging in Cardiac Amyloidosis: Part 1 of 2—Evidence Base and Standardized Methods of Imaging. Circ Cardiovasc Imaging 2021;14(7):e000029.
63. Chacko L, Kotecha T, Ioannou A, et al. Myocardial perfusion in cardiac amyloidosis. Eur J Heart Fail 2024;26(3):598–609.
64. Kass M, Haddad H. Cardiac allograft vasculopathy: pathology, prevention and treatment. Curr Opin Cardiol 2006;21(2):132–137.
65. Velleca A, Shullo MA, Dhital K, et al. The International Society for Heart and Lung Transplantation (ISHLT) guidelines for the care of heart transplant recipients. J Heart Lung Transplant 2023;42(5):e1–e141.
66. Miller CA, Sarma J, Naish JH, et al. Multiparametric cardiovascular magnetic resonance assessment of cardiac allograft vasculopathy. J Am Coll Cardiol 2014;63(8):799–808.
67. Korosoglou G, Osman NF, Dengler TJ, et al. Strain-encoded cardiac magnetic resonance for the evaluation of chronic allograft vasculopathy in transplant recipients. Am J Transplant 2009;9(11):2587–2596.
68. Karamitsos TD, Ntusi NA, Francis JM, Holloway CJ, Myerson SG, Neubauer S. Feasibility and safety of high-dose adenosine perfusion cardiovascular magnetic resonance. J Cardiovasc Magn Reson 2010;12(1):66.
69. Seitz A, Kaesemann P, Chatzitofi M, et al. Impact of caffeine on myocardial perfusion reserve assessed by semiquantitative adenosine stress perfusion cardiovascular magnetic resonance. J Cardiovasc Magn Reson 2019;21(1):33.
70. Ta AD, Hsu LY, Conn HM, et al. Fully quantitative pixel-wise analysis of cardiovascular magnetic resonance perfusion improves discrimination of dark rim artifact from perfusion defects associated with epicardial coronary stenosis. J Cardiovasc Magn Reson 2018;20(1):16.
71. Maredia N, Radjenovic A, Kozerke S, Larghat A, Greenwood JP, Plein S. Effect of improving spatial or temporal resolution on image quality and quantitative perfusion assessment with k-t SENSE acceleration in first-pass CMR myocardial perfusion imaging. Magn Reson Med 2010;64(6):1616–1624.
72. Otazo R, Kim D, Axel L, Sodickson DK. Combination of compressed sensing and parallel imaging for highly accelerated first-pass cardiac perfusion MRI. Magn Reson Med 2010;64(3):767–776.
73. Thornton GD. Bennett JB Nitsche C, et al. Myocardial Hypoperfusion in Severe Aortic Stenosis is Reversed by Aortic Valve Replacement. JACC Cardiovasc Imaging 2024;17(8):1006–1008.
74. Gulati A, Ismail TF, Ali A, et al. Microvascular Dysfunction in Dilated Cardiomyopathy: A Quantitative Stress Perfusion Cardiovascular Magnetic Resonance Study. JACC Cardiovasc Imaging 2019;12(8 Pt 2):1699–1708.
75. Gyllenhammar T, Kanski M, Engblom H, et al. Decreased global myocardial perfusion at adenosine stress as a potential new biomarker for microvascular disease in systemic sclerosis: a magnetic resonance study. BMC Cardiovasc Disord 2018;18(1):16.